

## INFORMATION TO USERS

The most advanced technology has been used to photograph and reproduce this manuscript from the microfilm master. UMI films the text directly from the original or copy submitted. Thus, some thesis and dissertation copies are in typewriter face, while others may be from any type of computer printer.

The quality of this reproduction is dependent upon the quality of the copy submitted. Broken or indistinct print, colored or poor quality illustrations and photographs, print bleedthrough, substandard margins, and improper alignment can adversely affect reproduction.

In the unlikely event that the author did not send UMI a complete manuscript and there are missing pages, these will be noted. Also, if unauthorized copyright material had to be removed, a note will indicate the deletion.

Oversize materials (e.g., maps, drawings, charts) are reproduced by sectioning the original, beginning at the upper left-hand corner and continuing from left to right in equal sections with small overlaps. Each original is also photographed in one exposure and is included in reduced form at the back of the book. These are also available as one exposure on a standard 35mm slide or as a 17" x 23" black and white photographic print for an additional charge.

Photographs included in the original manuscript have been reproduced xerographically in this copy. Higher quality 6" x 9" black and white photographic prints are available for any photographs or illustrations appearing in this copy for an additional charge. Contact UMI directly to order.

# U·M·I

University Microfilms International  
A Bell & Howell Information Company  
300 North Zeeb Road, Ann Arbor, MI 48106-1346 USA  
313/761-4700 800/521-0600



**Order Number 9000025**

**Fourier transform infrared studies of semicrystalline  
trans-1,4-polyisoprene**

**Gavish, Michal, Ph.D.**

**City University of New York, 1989**

**Copyright ©1989 by Gavish, Michal. All rights reserved.**

**U·M·I**  
300 N. Zeeb Rd.  
Ann Arbor, MI 48106



FOURIER TRANSFORM INFRARED STUDIES OF  
SEMICRYSTALLINE TRANS-1,4 POLYISOPRENE

by

Michal Gavish

A dissertation submitted to the Graduate Faculty  
in Chemistry as a partial fulfillment of the  
requirements for the degree of Doctor of Philosophy  
The City University of New York.

1989

COPYRIGHT BY  
MICHAL GAVISH

· 1989

This manuscript has been read and accepted for the Graduate Faculty in Chemistry in satisfaction of the dissertation requirement for the degree of Doctor of Philosophy.

10/6/88  
date

Arthur E. Woodward  
Chairman of Examining Committee

10/6/88  
date

J. H. [Signature]  
Executive Officer

[Signature]

[Signature]  
Supervisory Committee

The City University of New York

## Abstract

FOURIER TRANSFORM INFRARED STUDIES OF  
TRANS-1,4-POLYISOPRENE LAMELLAS

by

Michal Gavish

Advisor: Professor Arthur E. Woodward

The semicrystalline structure of trans-1,4-polyisoprene (TPI) lamellas was studied by FTIR spectroscopy. The crystalline and amorphous components of the spectrum were separated and assigned. The crystalline component was assigned for both the monoclinic (alpha) and the orthorhombic (beta) forms using normal coordinate calculations for a single chain. The calculations for the two crystal forms were compared and a correlation was found between both their frequencies and potential energy distribution. Each band in the beta spectrum was correlated to a singlet or a doublet in the alpha spectrum. Correlation

of each band in the spectra of the two crystalline forms with the amorphous spectrum was then used to assign the infrared bands of the latter. Conformational assignment for the different components of some of the amorphous bands were obtained using samples at different temperatures above the crystalline melting point.

Infrared studies of partially modified TPI lamellas were carried out. TPI lamellas were reacted in suspension so that the surfaces were modified and the crystalline cores remained unchanged. The reactions used were epoxidation, hydrochlorination and hydroxylation of the double bond. The infrared spectra of the modified surface were obtained and tentative assignment of the bands was made.

FTIR spectra of TPI were used to develop a method for the direct measurement of sample crystallinity. The effect of temperature on the lamellar structure was also studied and the sample crystallinity was found to increase by about 10% upon cooling from room temperature to  $-30^{\circ}\text{C}$ . The spectra also indicated changes with temperature in the crystalline interchain distances.

## ACKNOWLEDGEMENTS

I would like to express my thanks to Professor Arthur E. Woodward for his guidance and help throughout my studies.

I also wish to thank Dr. Nan-Loh Yang, Dr. Vernon Box and Dr. Ruth Stark for their help and encouragement.

## TABLE OF CONTENTS

	Page
I. Introduction.....	1
II. Experimental .....	22
Sample preparation.....	22
FTIR spectroscopy.....	24
Normal coordinate calculations.....	25
Surface reactions.....	28
Crystallinity measurements.....	32
Temperature effect on TPI spectra.....	33
III. Normal coordinate calculations.....	37
IV. Results.....	43
Infrared spectra of crystalline TPI.....	43
Assignment for amorphous band components.....	59
Surface modification.....	62
Crystallinity measurements.....	78
TPI spectra at low temperatures.....	83

V.	Discussion.....	93
	Assignment of TPI crystalline spectra.....	93
	Assignment of TPI amorphous spectrum.....	103
	Surface reactions.....	113
	Crystallinity measurements from ir spectra.....	122
	TPI spectra at low temperatures.....	130
VI.	References.....	138

## LIST OF TABLES

Table	page
1. Geometric parameters of TPI.....	27
2. Valence force constants for TPI.....	29
3. Correlation of observed and calculated alpha and beta TPI infrared frequencies.....	47
4. Correlation of the observed crystalline and amorphous infrared frequencies.....	53
5. Infrared frequencies and band component assignments for TPI in the melt.....	63
6. Infrared frequencies and band assignments for amorphous epoxidized and hydrochlorinated TPI...	69
7. Infrared frequencies and band assignments for hydroxilated TPI.....	77
8. Crystallinity of solution grown TPI lamellar samples.....	81

## LIST OF FIGURES

figure	page
1. Alpha trans-1,4 polyisoprene.....	3
2. Beta trans-1,4 polyisoprene.....	4
3. Polyisoprene repeat unit.....	26
4. Cooling cell.....	35
5. Spectrum of semicrystalline TPI.....	44
6. Spectra of crystalline and amorphous TPI.....	45
7. Correlation of spectral bands.....	58
8. Spectra of TPI at high temperatures.....	60
9. Changes in TPI spectra at high temperatures....	61
10. Spectrum of epoxidized TPI.....	65
11. Spectrum of hydrochlorinated TPI.....	66
12. Spectra of modified TPI lamellar surface.....	67
13. Spectrum of hydroxylated TPI.....	75
14. Digital subtraction of TPI spectra.....	79
15. Crystallinity measurements.....	84
16. Alpha TPI spectrum at low temperatures.....	85
17. Beta TPI spectrum at low temperatures.....	87

18.	Changes in alpha TPI spectrum at low temperatures	88
19.	Changes in beta TPI spectrum at low temperatures	89
20.	Subtraction of an amorphous component from TPI spectra at low temperatures.....	92
21.	Conformations of TPI repeat unit.....	97
22.	Methylene bending.....	134

## INTRODUCTION

Trans-1,4-polyisoprene, TPI, precipitates from dilute solutions as single lamellas with crystalline cores and amorphous surfaces (1,2) or as multilamellar structures (3,4) depending on the crystallization conditions. The morphology of these structures was determined using light and electron microscopy. Various morphologies were obtained for TPI (2): i) Single overgrown lamellas of elongated hexagonal morphology. ii) Curved overgrown lamellas. iii) Aggregates of cup shaped lamellas. iv) Spherulites. v) single overgrown lamellas with pointed ends.

The crystalline core and the amorphous surface of these structures were investigated by various methods. Two distinct crystalline forms were identified for this polymer, depending on the crystallization conditions. The alpha form was shown by X ray diffraction (5) to have a monoclinic unit cell with a  $P2_1$  space group having a  $C_{2h}$  symmetry. The cell contains two chains, each with two chemical repeat units

(Figure 1). The beta form has also been characterized by X ray diffraction (6). It has an orthorhombic unit cell with four chains passing through it, each containing one chemical repeat unit, with a  $P_{222}$  space group and a  $D_2$  symmetry (Figure 2). Methods were developed to prepare partially crystalline samples which contain either exclusively one crystalline form, the alpha or the beta, or samples in which both crystal forms are present (3). The crystalline components were also characterized by DSC (3) which gave different endotherms for the two crystal forms.

The structure of solution crystallized TPI has been investigated. Quantitative chemical reactions in suspension coupled with carbon 13 NMR (7,8) were used to determine the number of repeat units per average fold length and the crystalline stem length in the lamellas. TPI is well suited for this type of study due to the susceptibility of the double bond present in each repeat unit to addition reactions. Considerable effort has been expended in order to establish reaction conditions that lead to complete reaction of the lamellar surface only without penetration and

Figure 1      ALPHA TRANS-1,4 POLYISOPRENE

The conformations of the chains in a crystallographic unit cell of alpha trans-1,4 polyisoprene.

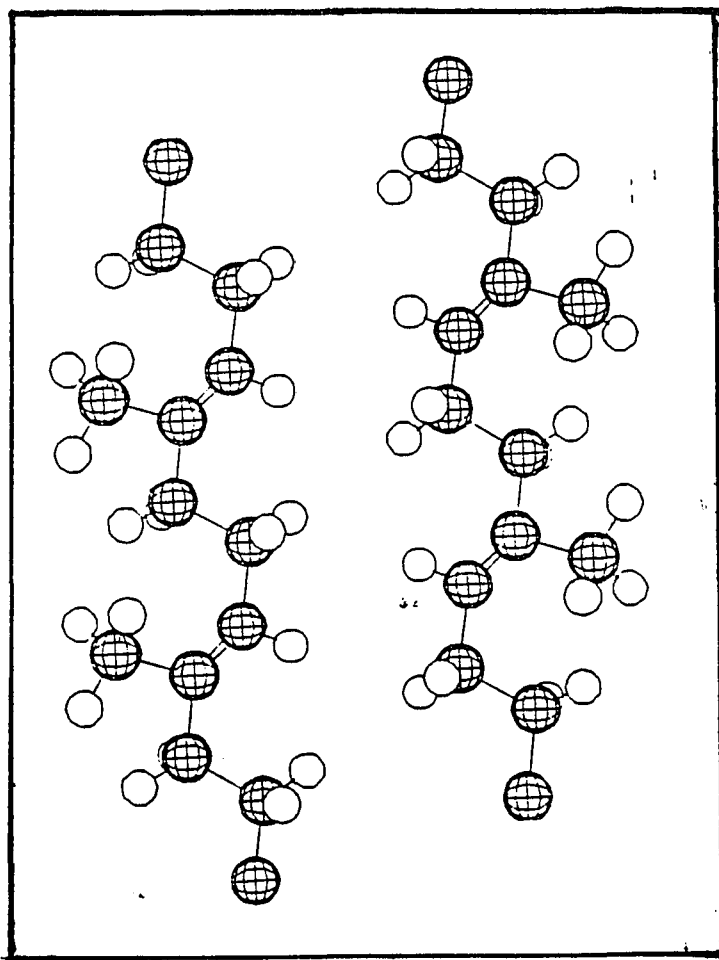
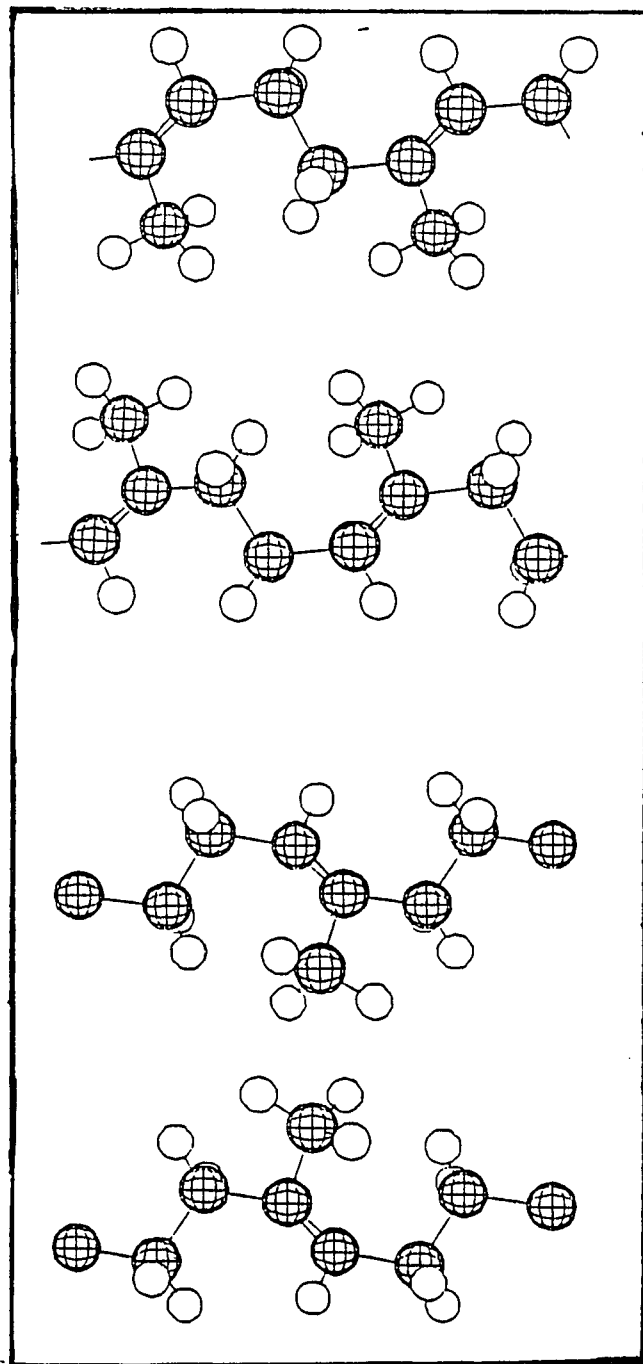


Figure 2      BETA TRANS-1,4 POLYISOPRENE

The conformations of the chains in a crystallographic unit cell of beta trans-1,4 polyisoprene.



reaction in the crystal core taking place to an appreciable degree. Two reactions for the modification of TPI have been investigated to date, epoxidation using m-chloroperbenzoic acid (7) and hydrochlorination of the double bond with hydrogen chloride gas (8). It has been shown that both of these reactions can be carried out under conditions that give single products and preserve the stereochemistry of the double bond, as characterized by carbon 13 NMR (7,8). When one or the other of these reactions goes to completion at the lamellar surfaces of solution crystallized TPI structures in suspension, the product which results has chemically modified blocks alternating with unmodified blocks (9).

Density measurements were used in order to quantitatively establish the relative amounts of the crystalline and the amorphous components of the trans-1,4 polyisoprene lamellas (10). This method was reviewed by Wunderlich (11). The crystallinity is calculated from the measured density and from values for the totally amorphous and the totally crystalline TPI samples (12,13). The results of these

measurements were used in order to confirm the crystalline and amorphous fractions obtained by other methods. Some disagreement in the values of crystalline density for beta TPI (7,8,10) has appeared; therefore the development of an alternative method to measure crystallinity was desirable.

It was of interest to explore the application of Fourier transform infrared spectroscopy (FTIR) to the characterization of the crystalline and noncrystalline components in solution crystallized TPI lamellas. The FTIR method was chosen because of its many advantages (14,15) :

1) The direct observation of the solid polymer by this method is experimentally simple.

2) Infrared spectroscopy is very sensitive to conformational changes in a sample since these can cause shifts in band frequencies. 3) The FTIR technique provides a very high signal to noise ratio and very accurate frequency readings. The accuracy, which is the result of the calibration by an He-Ne laser, makes it possible to add spectra of the same sample and to increase the signal to noise ratio even further. These special features, which do

not exist in continuous wave spectrometers can be used to follow subtle changes in the polymer structure as they are reflected in the spectrum. 4) The computer that is used to collect the data in FTIR spectrometer can be used for spectral manipulation and storage. In this way, various spectral components can be separately studied by methods such as subtraction, deconvolution and derivitization.

Infrared spectroscopy had been used extensively for the study of polymers and the identification of their structure. This method had been applied to polyisoprene in several works. In 1949 Saunders and Smith (16) reported and analyzed continuous wave spectra of polyisoprene. They identified both the most distinct bands that are unique to the cis and the trans isomers, and the bands that could distinguish between the alpha and the beta semicrystalline samples of TPI. In the same work a tentative assignment was given to many of the bands and orientation data were obtained from polarized infrared light experiments. In 1950, Sutherland and Jones (17) suggested a somewhat different assignment, mainly concerned with the vinyl CH group in and out of the

plane deformations and for some of the CH<sub>3</sub> modes. Another work (18) had also suggested that bands such as the 1130 and 1150 cm<sup>-1</sup> could be used to distinguish between the cis and the trans isomers respectively. The 1140 cm<sup>-1</sup> band was employed to characterize the 3,4 polyisoprene isomer (19). In 1963 Binder (20) studied purer cis and trans-polyisoprene samples and his assignments disagree with those made in previous studies. However, his work does not attempt to distinguish the crystal forms of each isomer. A later study (21) clearly identifies many of the crystalline bands and uses a larger set of bands to distinguish between the crystal forms of the trans isomer. In 1970 Golub (22) published a detailed analysis of cis-polyisoprene bands based on isotopic substitution data. Raman spectra of polyisoprene were reported (23) and band assignments based on past infrared work were made. Finally, the most extensive analysis for trans-polyisoprene was done using normal modes calculations (24). In that work, the assignment was essentially complete for the beta TPI spectrum but for alpha TPI not all the bands were assigned and some of the

calculated frequencies did not have an observed counterpart.

In the present work, normal coordinate calculations for a single chain was used to assign all the crystalline bands in both alpha and beta TPI spectra. The crystalline spectra that were obtained in this work had a very clear baseline with separate and sharp bands, some of which were different from those reported previously (24). The calculated frequencies and their potential energy distribution assignments differed from the previous calculations (24) for both crystal forms and agreed with assignments made in the earlier works (16,17).

As the spectral assignment for crystalline TPI progressed it was realized that a correlation existed between the observed infrared spectral frequencies for the two crystal forms. Each vibrational band in the spectrum for the beta form is correlated to a singlet in a few cases and a doublet in the majority of cases in the alpha spectrum. The correlated alpha and beta bands have the same or similar potential energy distribution assignment.

A method which is extremely useful for the analysis

and understanding of semicrystalline polymer spectra was developed by Koenig (25) to separate the spectrum of a two phase material. This method can be used to obtain a spectrum for the crystalline component from a spectrum for the semicrystalline polymer. The subtraction was illustrated by Koenig mathematically. According to this treatment, a semicrystalline spectrum has a total absorbance,  $A_t$  which is composed of three components: the crystalline absorbance bands  $A_c$ , the amorphous bands,  $A_a$ , and absorbance bands which are independent of conformation,  $A_i$ .

$$A_t(\nu) = A_c(\nu) + A_a(\nu) + A_i(\nu)$$

When two samples, I and II are subtracted their difference spectrum is expressed by:

$$A_t(\nu)_I - A_t(\nu)_{II} = (A_c(\nu)_I - kA_c(\nu)_{II}) + (A_a(\nu)_I - kA_a(\nu)_{II}) + (A_i(\nu)_I - kA_i(\nu)_{II})$$

Where  $k$  is the subtraction factor. In order to obtain a 100% crystalline spectrum, the subtraction factor must be chosen so that the amorphous absorbance term will vanish:

$$A_a(\nu)_I - kA_a(\nu)_{II} = 0$$

In this way the subtracted spectrum shows only the crystalline contribution from both the conformationally dependent and independent bands. In particular the properly scaled spectrum for a 100% amorphous sample is subtracted from that for the semicrystalline sample; the amorphous spectrum is easily obtained experimentally at a temperature above the melting point. The 100% amorphous spectrum has been shown to exhibit the same conformational distribution and the same infrared spectrum as the lamellar surface component (26). Subtraction has been carried out in this way for many polymers (27,28,29). The resulting spectrum for the crystalline component usually contains a good base line with sharp, separate distinct peaks. The broad bands which are normally associated with the amorphous absorption disappear from the spectrum upon subtraction. The choice of the subtraction factor,  $k$ , is done by following the disappearance of two or more distinct amorphous bands. The choice of a subtraction factor that is too large can be avoided since it would be indicated by the appearance of

negative components in the spectrum.

Vibrational spectra of many crystalline polymers have been assigned using normal coordinate calculations. These include polyethylene (30-32), polyolefins (33-35), haloethylenes (36-43), polydienes (24,44-47), polystyrene (48,49) and polyamides (50-53). In most cases the analysis was done using a single polymeric chain as a model for the geometric parameters and the force constants. However, some of the works (44,45,54,55) also include force field data for the chain-chain interactions. In these cases some terms are included in the force constant matrix and in the geometrical parameter matrix of atoms from adjacent chains that are close enough to other atoms to affect their vibrational modes. The results of the normal coordinate calculations were also verified by the use of many experimental techniques as follows: 1) For the same sample, the infrared and Raman spectra (45,46,56,57) were compared and assignments were shown to be consistent for modes which are expected by symmetry to be active or inactive in each spectrum. 2) Selective isotopic substitution (33,47,58) of

mainly  $^2\text{H}$  was used to show that a vibrational mode belongs to a particular functional group in the molecule. However, this method is limited because it could not distinguish between the vibrational modes of the same functional group, as for example, between the rocking, twisting and wagging modes for a methylene group. 3) Polarization data (33,47,48,58) were used to establish some of the assignments for bands with intensities which depended on their orientation.

The calculations for disordered polymers are complicated by the large number of conformations of the chemical repeat units in that state. Since sequential repeat units are not related to each other in any ordered pattern, coupling does not occur between their vibrational modes and repeat conformational units whose energy is invariant under translation can not be identified. The disordered part of the molecule must be treated by taking all its atoms into account which results in very large matrices. For this reason very few polymers were analyzed in this way. Zerbi and coworkers (59,60) developed a numerical method, based on

the negative eigenvalue theorem. However, this method was not applied to the analysis of the amorphous part in semicrystalline polymers but only to repeat units in the crystalline region which contained low concentration of amorphous component. This method was applied to polyethylene (61,62) but not all the amorphous bands were accounted for.

Most of the assignments for amorphous polymers have been carried out experimentally rather than by calculations. Snyder (30) attempted to analyze semicrystalline polyethylene. He treated the crystalline segments between the fold as finite and modified in this way the infinite chain calculations. In order to verify the assignments he used CD<sub>2</sub> units in polyethylene chains as conformational probes. Since vibrations were coupled to adjacent CH<sub>2</sub> units, any change in the latter caused a frequency shift in certain modes. In this work Snyder was able to identify sequences in liquid parafins but not for molten polymers where these modes collapsed into broad bands. Shimanouchi and coworkers (63) used small olefinic model compounds of known conformations. They have used the assignments of their bands

which were transferred to polyisoprene and polybutadiene. In another work (64) the rotation around the  $\text{CH}_2\text{-CH}_2$  bond in polybutadiene was determined from the  $1450\text{ cm}^{-1}$  band. The fold conformation was determined experimentally by heating the sample and assuming that the band components showing intensity increases are gauche-rich. In a similar study (65) Fourier self-deconvolution was used to identify fold band absorbances. This work has led to a direct proof of the adjacent fold theory in polymer lamellas. Jing and coworkers also studied (66) the fold structure in polyethylene lamellas using some deuterated units, and found an independent proof for the adjacent fold theory. A different approach was taken using low frequency Raman modes (67,68). These modes are sensitive to the number of sequential vibrating groups that are coupled to each other, or to the length of the ordered segments. Mazur et al (67) found gauche defects in ordered polyethylene in this way. Snyder (68) established quantitative measurements of the amorphous fraction in semicrystalline samples. In a different work (69) the conformational sequence in a fold was established

for n-alkanes that were identified by increasing n and causing "new folds" to appear.

In the present work the TPI amorphous spectral assignment was accomplished by correlation to the crystalline bands. The spectral frequency correlation that was found between the two crystalline TPI forms was extended to the bands in the amorphous spectrum. The relatively broad infrared amorphous bands are expected to overlap the corresponding crystalline ones since the conformation characteristic of the two crystalline forms are highly probable ones for the amorphous chains. This overlap can be used as a means of assignment by transferring it from the alpha and beta spectra to the amorphous one.

One method to study the conformational structure of a polymer chain in the lamellar surface is by assigning separate components of a broad amorphous band to different conformations. These separate components appear and disappear upon heating the sample to temperatures above  $T_m$ . This was done by Koenig and coworkers (71) for poly (vinyl chloride). In a different work (72,73) poly (ethylene

terphthalate) was studied at temperatures up to 468K. The trans and gauche conformations were identified in the infrared band contours. The effect of temperature changes in atactic polystyrene (74) was studied and two transitions were found, the higher one involved conformational changes that can be seen by changes in the band contours. The conformational structure in polyethylene was also studied using temperature changes and following the appearance of some new conformational sequences at 77K. For poly (tetrafluoroethylene) (75) the disappearance of some of the band components was also used to deduce the disappearance of some conformations.

The components of the amorphous bands in TPI were studied for the first time in this work. The polymer was heated to temperatures above its melting point and the changes that occur in the relative intensities of the broad band contours were used to assign the different components of these bands.

These studies were extended to low temperature regions in order to learn more about the spectra and the polymer

structure. This type of work had been carried out before for other polymers. In all the studies an increase in the bands intensities is observed as the sample temperature is decreased. Two works on polyethylene (76) and polystyrene (77) show that there is a linear change that occurs for these amorphous polymers in their extinction coefficient, this can be expressed by:

$$e = e(T_r) + a(T - T_r)$$

where  $T_r$  is a reference temperature and  $a$  is the linear factor. The authors of these studies explain these changes as rising from intermolecular contraction which leads to an increase in the dipole moment interaction and therefore to an increase in the intensity. This phenomenon was found to be most pronounced for highly polar groups. Changes in the slope of the graph of temperature versus intensity indicated the occurrence of a transition. The same type of studies were done (74) on polystyrene at low temperatures where transitions for the sample were also observed. A slightly different explanation was given of the temperature increase by K. W. Frank and coworkers who studied polyethylene,

polyetyleneterphthalate and polyurethanes (78,79). They explained the increase in absorbance peaks intensity as resulting from anharmonicity that occurs as the lattice potential decreases and vibrational force constants increase. Another work (80) showed that small frequency shifts are expected at low temperatures for the same reason. Intensity band increases were also shown by Boerio (75) who indicated that with the increase in intensity some narrowing in the bands occur.

Since the different spectra of the crystalline and amorphous components of TPI were clearly established, these could be used to determine the relative amounts of these two components, which are related to the sample crystallinity. Some measurements of crystallinity have been carried out for a few polymers using their infrared spectra (11,81,82). However, the methods for these measurements were not direct since the results were not obtained from the bands themselves but from a plot that involves extrapolation to values for 100% crystalline or 100% amorphous samples. In other works (83) crystalline bands were identified and the

measurements of their intensity led to an approximation of the sample crystallinity. Also, in a similar way, low frequency Raman modes were used to measure the amorphous fraction in semicrystalline samples (68).

In this work (84) a new procedure was developed to obtain sample crystallinity from the C=C stretching band for TPI spectrum. A separate work describes (85) a similar method of obtaining the crystallinity fraction from all the bands in the spectrum simultaneously. This method had been applied in this work to TPI samples whose crystalline density was determined as a function of temperature.

## THE OBJECTIVES OF THE PROPOSED RESEARCH

The principal goal of this work is to apply the use of infrared spectroscopy for the study and the characterization of the different components of the semicrystalline structure of solution grown TPI lamellas. To meet this goal the following work was carried out:

- 1) FTIR spectra were obtained for the different components of semicrystalline TPI.
- 2) An assignment was made for the crystalline and amorphous spectra of TPI as well as for the components of some amorphous bands.
- 3) Infrared spectra for partially modified TPI lamellas were obtained and tentatively assigned.
- 4) A glycolated TPI block copolymer was prepared and characterized by infrared spectroscopy.
- 5) A method for crystallinity measurements from infrared spectra was developed. These measurements were applied to TPI samples at different temperatures.
- 6) Changes in TPI lamellar structure at low temperatures were observed by following the changes in the infrared spectra taken at those temperatures.

## EXPERIMENTAL

### SAMPLE PREPARATION

Trans- 1,4-polyisoprene (TPI) was crystallized from dilute solutions into semicrystalline lamellas with a crystalline core of either the alpha or the beta form. To obtain the beta crystalline form, the following procedure was used (4): Synthetic unfractionated TPI ( $M_w = 1.7 \times 10^5$ ,  $M_w/M_n = 4.8$ ) was precipitated from 1% amyl acetate solution at 0°C, followed by slow heating in the crystallization liquid to 30°C. The crystals were left at 30°C for one day. The suspension was diluted with fresh liquid and observed using a Zeiss light microscope. A morphology of curved stacks of overgrown lamellas was evident. Unfractionated Balata ( $M_w = 2.2 \times 10^5$ ,  $M_w/M_n = 4.3$ ) was crystallized by the same procedure as that above. In this case the resulting morphology was aggregates of cup shape lamellas. Unfractionated Gutta Percha ( $M_w = 2.7 \times$

$10^5$ ,  $M_n/M_w = 4.3$ ) was crystallized using the same method and resulted in a spherulitic morphology.

The synthetic material was also used to obtain samples with a crystalline core of the alpha form by two methods (3):

1) A solution of 0.5% (w/v) synthetic TPI in amyl acetate was cooled directly to a temperature of 30°C and crystals were grown isothermally for three days. The resulting suspension showed a spherulitic morphology. 2)

Unfractionated synthetic samples were also crystallized using the precooling method. The samples were precipitated from 0.1% (w/v) hexane solution at 0°C, redissolved at 32°C and crystallized isothermally at 20°C for two days. This resulted in semicrystalline overgrown single lamellas with an ellipsoidal shape and pointed ends. All samples were washed with fresh solvent and lamellar mats were formed by filtration of the suspension onto teflon filters and drying at room temperature.

## FTIR SPECTROSCOPY

Fourier transform infrared spectra were obtained for all samples using a Digilab FTS40 spectrometer. Room temperature spectra for semicrystalline samples with crystalline phase of either the alpha or the beta form were obtained. The FTIR spectra from 450 to 4000  $\text{cm}^{-1}$  were recorded with a resolution of 4  $\text{cm}^{-1}$  and 16 scans. The amorphous spectrum was taken for a TPI sample heated above the melting point to 65°C. The spectra were taken from 500 to 4000  $\text{cm}^{-1}$  with 16 scans. All the sharp bands which were associated with crystalline vibrations disappeared at this temperature, leaving a spectrum which contained broad bands only. This amorphous spectrum was used to obtain 100% crystalline spectra by digitally subtracting it from spectra of semicrystalline samples, with a crystal core of either alpha or beta crystalline form. For the alpha crystalline spectrum the sample obtained by method 1 above was used. For the beta crystalline spectrum sample prepared from synthetic material was employed.

## NORMAL COORDINATE CALCULATIONS

Normal coordinate calculations were carried out for TPI single chains in each of the two stable crystalline forms using a computer program written by Boreo (86) . The molecular parameters for carbon atoms in the alpha and beta TPI crystal structures were taken from earlier X-ray diffraction studies (5,6) and are summarized in Table I. The spatial arrangement for the hydrogen atoms was approximated by assuming the completion of a tetrahedral arrangement around single bonded carbons and a trigonal arrangement around the double bonded ones. The normal coordinates for these structures, which were defined in Figure 3, were transferred into cartesian coordinates using a computer program (87). The force constant data for the alpha and beta conformational repeat units were constructed by a valence force field transferred from model compounds. Most of the force constants involving chain backbone vibrations as well as those for the methylene coordinates were transferred from trans-1,4-polybutadiene (44). The force constants for the methyl group vibrations as well as

Figure 3 POLYISOPRENE REPEAT UNIT

The normal coordinates in trans-1,4 polyisoprene.

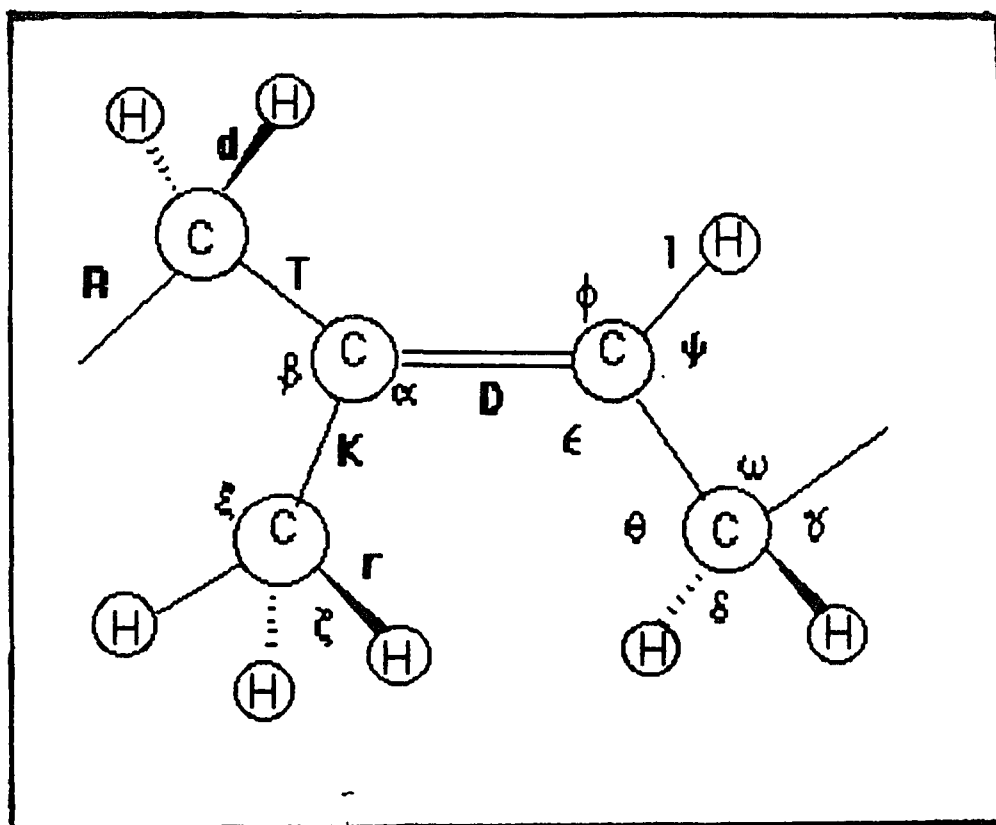


**Table I**  
**Geometric Parameters of TPI**

$C(4a)-[-C(1)-C(2)=C(3)-C(4)-]C(5)-[-C(1')-C(2')=C(3')-C(4')-]C(5')$					
Bond length (Å)	Bond angle, $\psi$ ( $^\circ$ )		Dihedral angle, $\tau$ ( $^\circ$ )		
$\alpha$ TPI					
C=C	1.38	$\psi_{123}; \psi_{1'2'3'}$	126.5	$\tau_{1234}; \tau_{1'2'3'4'}$	180
C-C	1.53	$\psi_{234}; \psi_{2'3'4'}$	124.8	$\tau_{2341}; \tau_{2'3'4'1'}$	8.6
C-H	1.09	$\psi_{341}; \psi_{3'4'1'}$	111.4	$\tau_{341'2'}$	179.0
		$\psi_{4a12}; \psi_{4'1'2'}$	107.6	$\tau_{4a123}$	111.0
		$\psi_{235}; \psi_{2'3'5'}$	125.2	$\tau_{41'2'3'}$	-111.0
		$\psi_{534}; \psi_{5'3'4'}$	120		
		HCH	109.5		
		CCH	109.5		
		C=CH	120		
$\beta$ TPI					
C=C	1.33	$\psi_{123}$	120	$\tau_{1234}$	180
C-C	1.54	$\psi_{234}$	125	$\tau_{4a123}$	117
C-H	1.09	$\psi_{341'}$	109.5	$\tau_{2341'}$	-117
		HCH	109.5	$\tau_{341'2'}$	180
		CCH	109.5		
		C=CH	120		

those involving the double bond were transferred from trans- and cis-butene (88,89) and from polypropylene (33). The force constants, as shown in Table II were applied to both the alpha and beta structure.

#### SURFACE REACTIONS

TPI lamellas with a beta core (synthetic) and with an alpha crystalline core (sample #1) were partially modified. Each sample was separately suspended in n-butanol in an excess of 3/1 of m-chloroperbenzoic acid per available double bond. The samples were reacted at 0°C for three days (90).

A different portion of the alpha and beta - containing samples were suspended in acetone and allowed to react for seven days with gaseous hydrogen chloride which was dissolved in large excess in the suspension liquid at -7°C (8). An attempt was made to hydroxylate other portions of samples with alpha and with beta crystalline cores. The polymer was suspended in amyl acetate at room temperature for an hour with enough osmium tetroxide to modify the available double bonds. The reaction product was washed,

**Table II**  
**Valence Force Constants for TPI<sup>a</sup>**

Force constant	Value	Force constant	Value	Force constant	Value
$H_{\epsilon}$	0.910	$H_{\xi}^b$	0.611	$F_{K\xi}^c$	0.174
$H_{\beta}$	0.944	$H_{\delta}$	0.540	$F_{\theta\theta}$	-0.032
$\Gamma_1$	0.344	$H_{\phi}$	0.560	$F_{\theta\delta}$	0.015
$\Gamma_2$	0.199	$H_{\psi}$	0.480	$F_{\phi\psi}$	0.027
$\tau_D$	0.328	$\tau_T$	0.024	$F_{\epsilon\psi}$	-0.029
$F_{T\omega}$	0.419	$\tau_K^b$	0.0073	$F_{\omega\theta}$	-0.028
$K_T$	4.384	$F_{DT}$	0.094	$F_{\xi\xi}$	-0.031
$K_K^b$	4.672	$F_{TR}$	0.122	$F_{\theta\theta}^t$	0.010
$K_D^b$	7.901	$F_{dd}$	0.004	$F_{\theta\theta}^g$	-0.006
$K_R$	4.947	$F_{\pi}^b$	0.037	$F_{\delta\delta}^t$	0.120
$K_d$	4.524	$F_{D\psi}$	0.355	$F_{\delta\delta}^g$	-0.02
$K_r^c$	4.699	$F_{T\theta}$	0.341	$f_{\delta\theta}^t$	0.008
$H_{\omega}$	1.049	$F_{T\psi}$	0.333	$f_{\delta\theta}^g$	0.029
$H_{\delta}$	0.664	$F_{T\delta}$	0.066	$f_{\omega\omega}^t$	0.080
$H_{\theta}$	0.668	$F_{T\phi}$	0.075	$f_{\omega\delta}^t$	-0.045
$H_{\xi}^b$	0.529			$f_{\omega\delta}^g$	0.073
$K_T = K_R$	$F_{\delta\delta} = F_{\theta\theta}$	$F_{\epsilon\psi} = F_{\psi\epsilon}$	$f_{\theta\delta}^t = f_{\psi\delta} = f_{\phi\theta}$		
$H_{\alpha} = H_{\beta}$	$\tau_T = \tau_R$	$F_{\delta\delta}^t = F_{\psi\theta}$	$f_{\theta\delta}^g = f_{\phi\theta} = f_{\psi\delta}$		
$F_{T\delta} = F_{R\theta}$	$F_{\omega\delta} = F_{\omega\theta}$	$F_{\omega\omega} = F_{\epsilon\epsilon}$	$f_{\theta\theta}^g = f_{\delta\phi} = f_{\epsilon\omega}$		
$F_{T\epsilon} = F_{D\epsilon}$	$F_{T\phi} = F_{D\psi}$	$F_{\delta\delta}^g = F_{\psi\theta}$	$f_{\omega\delta} = f_{\epsilon\theta} = f_{\omega\psi}$		

Table II (continued)

<sup>a</sup>The symbols for force constant definitions are taken from ref 30. The symbols for the internal coordinates for TPI are shown in Figure 3. All stretch force constants are in mdy/A; stretch-bend interactions are mdy/rad; bend constants are in units of (mdyn-A)/rad<sup>2</sup>. Most force constants are transferred from *trans*-1,4-polybutadiene (ref 44) unless otherwise noted. <sup>b</sup>Force constants transferred from *trans*- and *cis*-butene (refs 88, 89). <sup>c</sup>Force constants transferred from polypropylene (ref 33).

filtered and dissolved in methylene chloride. This solution was combined with a 1% potassium hydroxide solution in water containing a 2/1 excess of mannitol per osmated double bond. The reaction was allowed to take place at room temperature for 30 days. The product was collected from the water/methylene chloride interface (91).

The modified samples were washed in fresh suspension liquid at the reaction temperature. Thin mats (0.001-0.003 inch) were prepared by filtering the suspended sample using teflon filters and drying at room temperature. FTIR spectra were obtained for all samples from 450 to 4000  $\text{cm}^{-1}$  with 16 scans and a resolution of 4  $\text{cm}^{-1}$ . After obtaining these spectra, the modified samples were pressed for 15 minutes using a pressure of 200  $\text{lb/in}^2$ . FTIR spectra were obtained for these samples using the same conditions as those for the unpressed samples. A spectrum of a 100% crystalline sample of either the alpha or the beta form, depending on the sample, was digitally subtracted from the partially modified samples spectra so that all the sharp crystalline TPI bands disappeared.

## CRYSTALLINITY MEASUREMENTS

Crystallinity measurements were done for all semicrystalline samples using their FTIR spectra. Additional samples were prepared from synthetic TPI with beta and alpha cores (sample #1). These samples were pressed for 15 minutes under a minimum readable pressure of 200 lb/in<sup>2</sup>. FTIR spectra were obtained for all samples at room temperature from 450 to 4000 cm<sup>-1</sup> with 16 scans and a resolution of 4 cm<sup>-1</sup>. An amorphous TPI spectrum was digitally subtracted from this spectrum and a 100% crystalline spectrum was obtained. The relative intensity of the C=C stretching band at 1664-1672 cm<sup>-1</sup> in the crystalline and semicrystalline normalized spectra of each sample was obtained from the band area by cutting and weighing.

The same samples were used for crystallinity measurements from density using a gradient column (10). The column contained alcohol and water which were mixed and layered so that the density increases linearly from the top to the bottom. The column was calibrated with glass beads

of known density. The sample crystallinities were calculated from the density values for amorphous (91) and for 100% crystalline (92) TPI.

#### TEMPERATURE EFFECT ON TPI SPECTRA

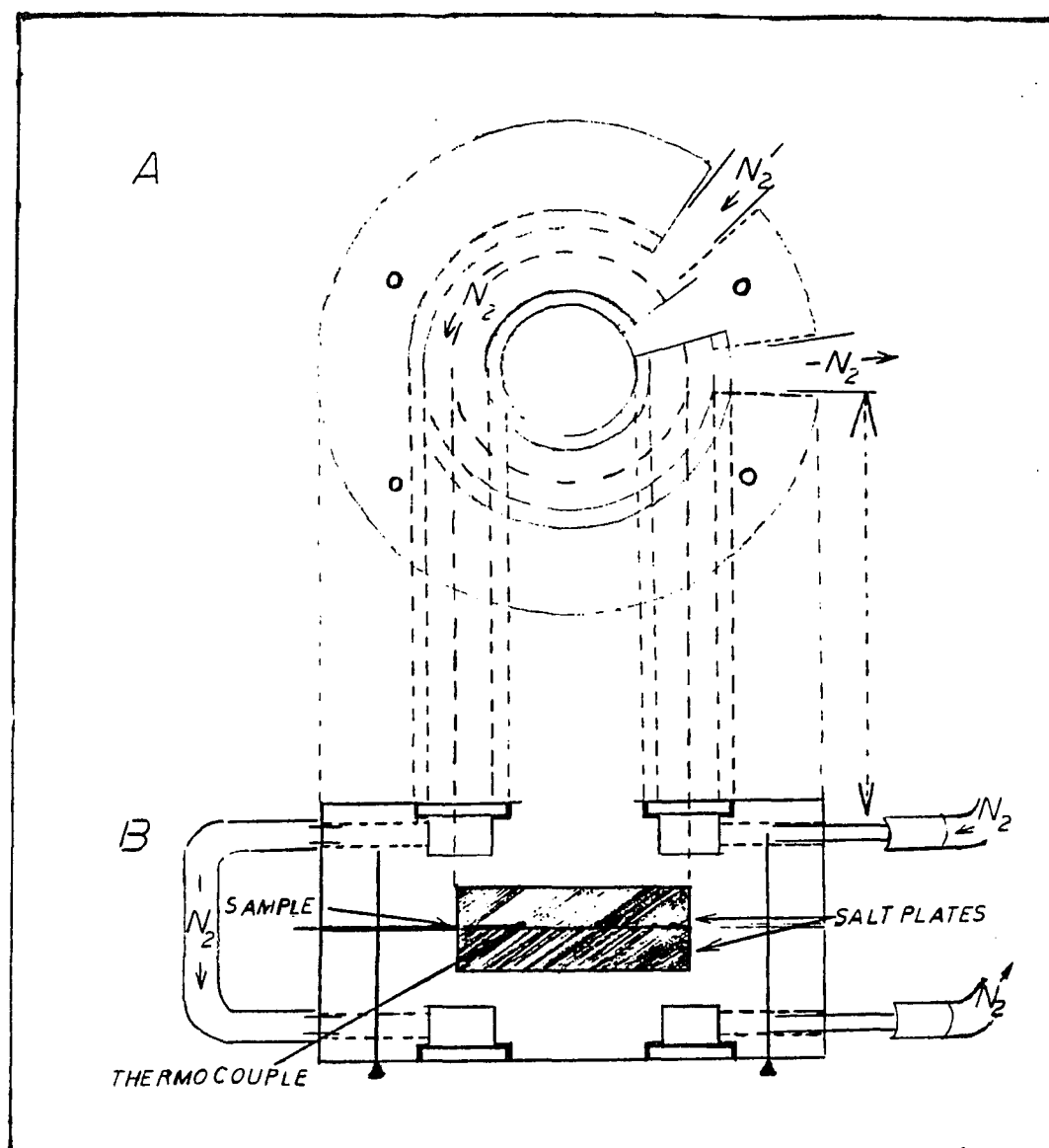
Semicrystalline samples with alpha and with beta crystalline cores were heated starting at room temperature using a thermostated heating cell (Model 48) made by Control Cooperation. The sample temperature was raised slowly by five degrees at a time and then kept constant while the FTIR spectra of the sample with 16 scans and a 4  $\text{cm}^{-1}$  resolution were recorded from 500 to 4000  $\text{cm}^{-1}$ . Spectra were obtained in this way from room temperature to 110°C. The same samples were used to obtain spectra upon cooling from 110°C to room temperature. The spectrum taken at each temperature was digitally subtracted from that taken at 110°C using a subtraction factor of one. The subtracted spectra were used for conformational analysis of amorphous TPI bands. The 100% amorphous spectrum taken at 65°C was subtracted from the spectra taken between ambient

temperature and 60°C, to obtain 100% crystalline spectra. The factor required for these subtractions changed with temperature; it was recorded and used for crystallinity measurements. Deconvolution of three amorphous bands at 1235-1205, 987-976 and 842 cm<sup>-1</sup> was also performed for the spectra taken at 65 and at 110°C.

The same type of samples were used for a cooling experiment. A cooling cell was designed (see Figure 4) from two cylindrical copper plates with a circular space that allows the vapor from liquid nitrogen to cool it. The sample was placed between two sodium chloride plates in the infrared beam path. A thermocouple was attached to the sample. The samples were cooled down to -145°C at a rate of about 5.5°C per minute and FTIR spectra recorded at temperature intervals of about 10°C. A spectrum of semicrystalline TPI taken at room temperature was subtracted, using a factor of one, from each of the spectra with the same crystal form taken at low temperatures in order to follow spectral changes. The same samples were warmed up at a rate of about 5°C per minute and their

Figure 4 COOLING CELL

A copper cooling cell designed for FTIR spectroscopy at low temperatures. A) Top view. B) Cross sectional view.



spectra were obtained at approximately 10°c intervals. In addition, an amorphous sample obtained at 65°c was subtracted from each of these spectra and the subtraction factor used for calculations of the sample crystallinity.

### NORMAL COORDINATE CALCULATIONS

Normal coordinate calculations are used in order to assign each crystalline band to one or more vibrational modes. The calculations for polymers are based on a method which was developed for small molecules (92,93). The molecular vibrations are simplified by separating them into a linear combination of normal vibrations. Each normal vibration is periodic around a certain normal coordinate. The vibrations are assumed to be harmonic, a good approximation for fundamental modes, and their energy is described by:

$$E = 1/2 h\nu$$

The vibrational motion is given by Newton's second equation of motion which includes a description of the potential energy,  $V$ , and the kinetic energy,  $T$ :

$$-\frac{d}{dt} \left( \frac{\partial T}{\partial \dot{q}_i} \right) + \frac{\partial V}{\partial q} = 0$$

The kinetic and the potential energy parts can be expressed separately as

$$2T = (\dot{x})^T (m) (\dot{x}) \quad \text{for the kinetic energy}$$

and

$$2V = (R)^T F_x (R) \quad \text{for the potential energy.}$$

The problem in solving these equations arises from the fact that the kinetic energy is most conveniently expressed by cartesian displacement coordinates while the potential energy is more easily written using internal coordinates, since the force constants are expressed along these coordinates. In order to solve the equation of motion both energies must be expressed by the same set of coordinates. The B matrix is used for the coordinate transformation:

$$Bx = R$$

Or, the coordinates can also be mass adjusted so that

$$B_m = BM^{-1/2}$$

and

$$R = B_m X$$

In this way, the G matrix is defined by:

$$G = B_m B_m'$$

The kinetic energy equation can now be expressed in terms of

internal coordinates, R:

$$2T = R G^{-1} R$$

and the potential energy becomes

$$2V = R F R$$

The solution for the equation of motion is obtained from the secular equation:

$$| GF - E | = 0$$

and  $\lambda = 4\pi^2 c^2 v^2$ , where  $c$  is the velocity of light and  $v$  the vibrational frequency in wave numbers.

In this way, if data are obtained for the geometries, masses and force constants of the molecule, the frequencies of vibration can be calculated.

Since polymers are very large molecules, the calculation of their vibrations, whose number is related to the number of their atoms, becomes very complicated. For this reason, crystalline polymers are considered as infinite chains containing repeat conformational units whose internal coordinates are related to each other by the screw dislocation operation under which the potential and kinetic energies are invariant. The normal vibrations would then be

expressed by a phase angle, theta, that represents the screw dislocation operation between adjacent repeat units. This was first given by Higgs (94):

$$R(\theta) = \sum R_n e^{i n \theta}$$

And was later applied and modified (95) to show that the energies for an infinitely long polymer chain could be expressed as:

$$G(\theta) = \sum G_n e^{i n \theta}$$

$$F(\theta) = \sum F_n e^{i n \theta}$$

The nontrivial solution for the secular equation is given by:

$$\begin{vmatrix} G(\theta) & F(\theta) \\ -\lambda(\theta) & E \end{vmatrix} = 0$$

where:

$$\lambda(\theta) = 4II^2 c^2 v^2(\theta)$$

This solution is now in terms of a continuous function rather than a discrete value. However according to the vibrational selection rules (94) for an infinite polymer chain, only integer multiples of the helix angle will be optically active and in this way, only the allowed values become the solution for the secular equation. For polymers

which are not helical, like for example those having zigzag configuration, the helix angle is simply taken as zero or  $180^\circ$ .

In addition to the frequencies of vibration, it is valuable to also calculate the potential energy distribution, PED, which expresses the percent contribution of the different force constants to a given normal vibration. This is derived from the fact that the PED can be expressed in terms of normal coordinates,  $Q$ :

$$2V = \lambda_i Q^2_i$$

The internal coordinates are also converted now into mass adjusted normal coordinates by using the  $L_q$  transformation matrix:

$$q = L_q Q$$

So that the direct transformation from the internal to normal coordinates is:

$$R = LQ$$

and the potential energy becomes:

$$2V = R'F R = Q'L'F L Q$$

But since also:

$$2V = Q' \wedge Q$$

then

$$L' F L = \wedge$$

or, if separate frequencies are described:

$$L_{j i} L_{k i} f_{j k} = \lambda_i$$

And the percentage distribution of each force constant'  $f_{j k}$

can be expressed as:

$$(\% \text{ PED}) = \frac{L_{j k} L_{k i} f_{j k}}{\lambda_i} \times 100$$

## RESULTS

### INFRARED SPECTRA OF SEMICRYSTALLINE TPI

The infrared spectra from 450 to 3100  $\text{cm}^{-1}$  of semicrystalline alpha and beta TPI taken at room temperature are shown in Figure 5. Each spectrum contains both sharp bands which are associated with the crystalline lamellar component and broad bands associated with the amorphous component. The amorphous spectrum from 500 to 3100  $\text{cm}^{-1}$  taken at 65°C contains only broad bands and is shown in Figure 6a. The 100% crystalline spectra shown in Figure 6b&c were obtained for alpha and for beta TPI, respectively, from 500 to 3100  $\text{cm}^{-1}$  by digital subtraction of the amorphous spectrum (Figure 6a) from the semicrystalline ones (Figures 5a& 5b). The subtraction was obtained by simultaneously observing the disappearance of the 842 and the 1099  $\text{cm}^{-1}$  bands and avoiding the appearance of negative components next to any of the bands in the spectrum. The baseline appeared very clear and each peak

Figure 5 SPECTRUM OF SEMICRYSTALLINE TPI

Infrared spectra of semicrystalline lamellar sample of trans-1,4 polyisoprene. A) with an alpha core. B) with a beta core.

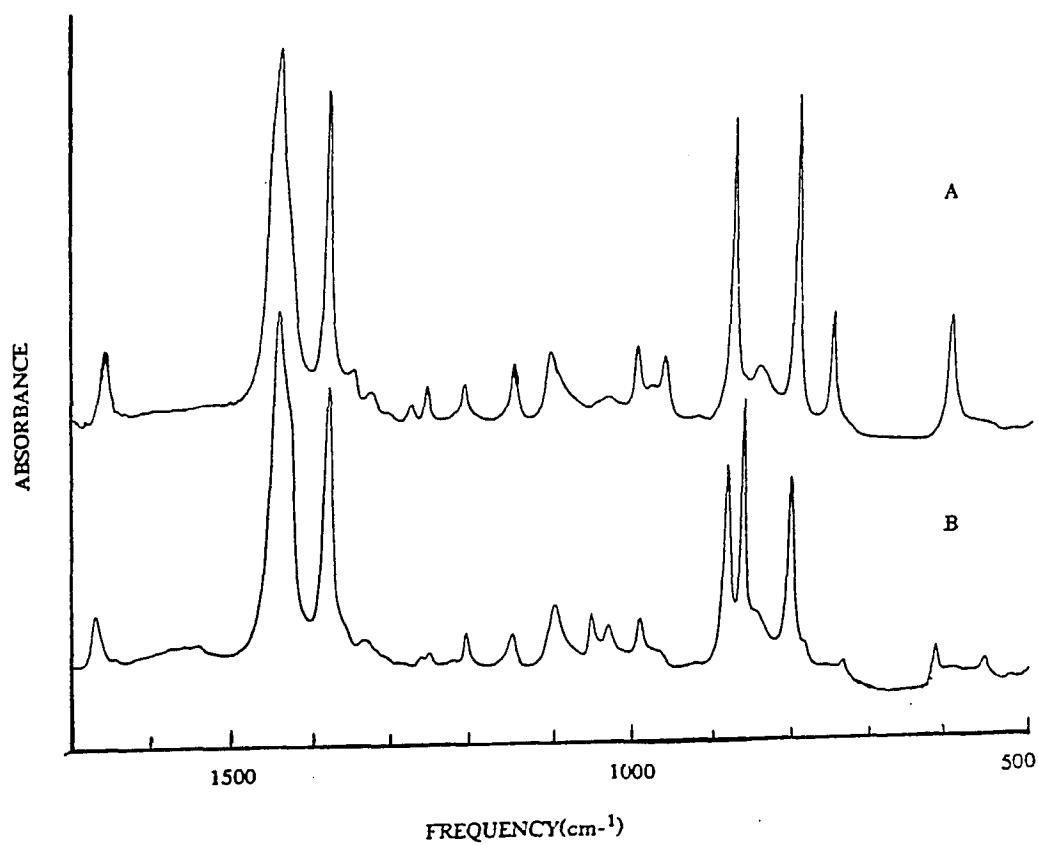
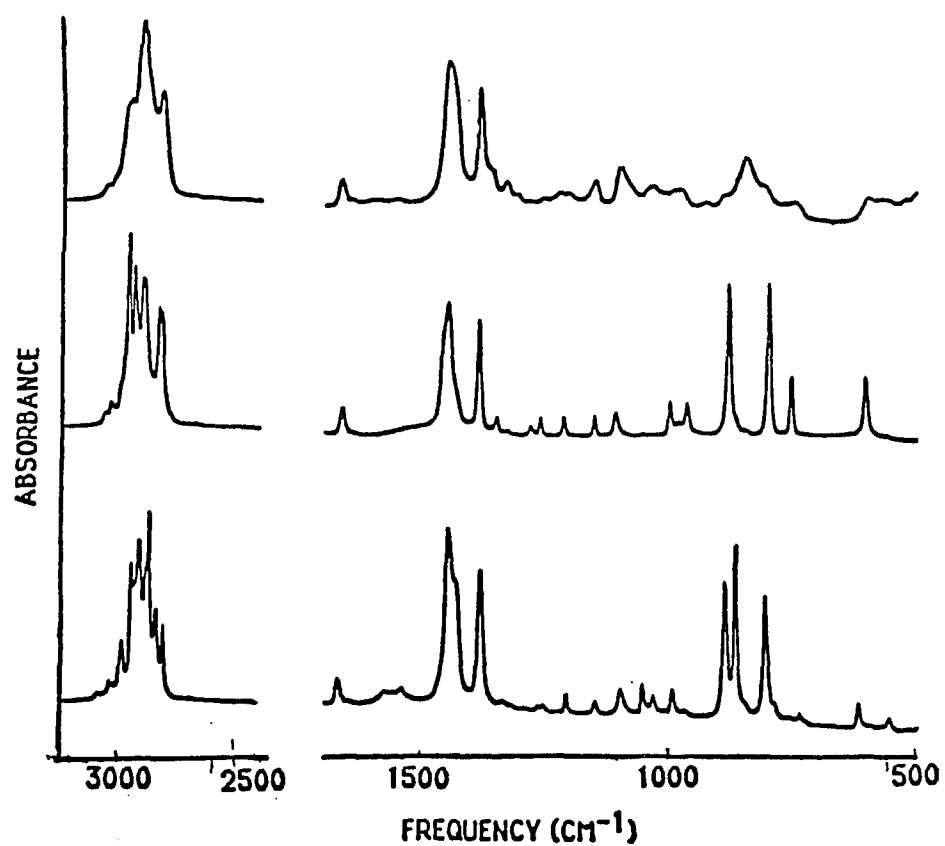


Figure 6 SPECTRA OF CRYSTALLINE AND AMORPHOUS TPI

Infrared spectra of the separate components of trans-1,4 polyisoprene lamellas. A) Amorphous TPI. B) Alpha TPI. C) Beta TPI.



was sharp and separate from the others. The alpha spectrum shows more bands than the beta spectrum. Differences between the observed crystalline and amorphous spectra in this and a previous FTIR study of TPI (24) are seen for both the alpha and the beta forms. Bands not observed in the previous study for a sample which was predominately alpha TPI appear at 2830 (s), 1250 (w), 780 (sh) and 555  $\text{cm}^{-1}$  (m). Other bands which were previously observed at 1010 and 604  $\text{cm}^{-1}$  are absent in the present work. It is to be pointed out that the 604  $\text{cm}^{-1}$  band reported earlier is characteristic of the beta form. For the beta form the bands at 2980  $\text{cm}^{-1}$  (sh) and 1058  $\text{cm}^{-1}$  (w) are observed in the present study and were not reported earlier.

The calculated frequencies for crystalline TPI from single chain analysis are given in Table III along with the observed bands in the 80 to 4000  $\text{cm}^{-1}$  region. This study shows close agreement ( $\pm 3-6 \text{ cm}^{-1}$ ) between the calculated and the observed frequencies for the C=C stretching band in the alpha (1672  $\text{cm}^{-1}$ ) and in the beta (1664  $\text{cm}^{-1}$ )

**Table III**  
**Correlation of Observed and Calculated  $\alpha$  and  $\beta$  TPI Infrared**  
**Frequencies**

$\beta$ TPI				$\alpha$ TPI		
Freq (cm <sup>-1</sup> )		P. E. D. <sup>a</sup>		Freq (cm <sup>-1</sup> )		P. E. D. <sup>a</sup>
obs	calc	(%)		obs	calc	(%)
3022	3019	99K <sub>1</sub>	—	3018	3018,3017	99K <sub>1</sub>
2979	2959	100K <sub>r</sub>	—	2970	2965,2965	100K <sub>r</sub>
2965	2957	100K <sub>r</sub>	—	2941	2963,2963	100K <sub>r</sub>
2943	2921	100K <sub>d</sub>	—	2918	2922,2923	100K <sub>d</sub>
2914	2918	100K <sub>d</sub>	—	2879	2914,2914	100K <sub>d</sub>
2906	2887	99K <sub>r</sub>	—	2872	2871,2868	99K <sub>r</sub>
2855	2847	99K <sub>d</sub>	—	2851	2850,2850	99K <sub>d</sub>
2846	2841	99K <sub>d</sub>	—	2830	2842,2841	99K <sub>d</sub>
1664	1670	72K <sub>D</sub> , 12K <sub>T</sub>	—	1672	1669,1670	72K <sub>D</sub> , 14K <sub>T</sub>
-	-			1579	1559	15 K <sub>T</sub> , 12K <sub>K</sub>
-	-			1540	1523	14 K <sub>T</sub> , 16K <sub>K</sub>
1450	1463	93 H <sub>z</sub>	—	1450	1469	71 H <sub>z</sub> , 18H <sub>z</sub>
	1463	91 H <sub>z</sub>			1463,1463	92H <sub>z</sub>
	1454	75 H <sub>z</sub>			1462,1462	92H <sub>z</sub>
					1460	75H <sub>z</sub> , 11H <sub>z</sub> , 11H <sub>z</sub>

Table III (continued)

$\beta$ TPI				$\alpha$ TPI		
Freq (cm <sup>-1</sup> )		P.E.D. <sup>a</sup>		Freq (cm <sup>-1</sup> )		P.E.D. <sup>a</sup>
obs	calc	%		obs	calc	%
1430	1446	77 H <sub>δ</sub>	—	1430	1448 1446	80H <sub>δ</sub> , 11H <sub>γ</sub> , 11H <sub>θ</sub> 80H <sub>δ</sub> , 10H <sub>γ</sub> , 12H <sub>θ</sub>
1384	1387	39 H <sub>ζ</sub> , 40 H <sub>ξ</sub>	—	1383	1377 1373	28H <sub>ζ</sub> , 32H <sub>ξ</sub> , 18H <sub>γ</sub> 41H <sub>ζ</sub> , 47H <sub>ξ</sub>
1348	1361	10 H <sub>ζ</sub> , 12 H <sub>ξ</sub> , 17K <sub>T</sub>	—	1340	1347	38H <sub>γ</sub> , 15H <sub>θ</sub> , 15H <sub>ζ</sub> , 17H <sub>ξ</sub>
1324	1335	61H <sub>γ</sub> , 18 H <sub>θ</sub> , 11I <sub>T</sub>	—	1320	1306	38H <sub>γ</sub> , 32H <sub>θ</sub>
1280	1322	45H <sub>γ</sub> , 40H <sub>θ</sub>	—	1280	1262 1256	42H <sub>γ</sub> , 51H <sub>θ</sub> 56H <sub>γ</sub> , 50H <sub>θ</sub>
1260	1252	44H <sub>γ</sub> , 45H <sub>θ</sub>	∧	1260	1248 1244	41H <sub>γ</sub> , 47H <sub>θ</sub> 47H <sub>γ</sub> , 49H <sub>θ</sub>
				1250	1235 1230	36H <sub>γ</sub> , 40H <sub>θ</sub> 52H <sub>γ</sub> , 43H <sub>θ</sub>
1212	1192	21H <sub>ψ</sub> , 24H <sub>θ</sub> , 10K <sub>T</sub> , 18H <sub>γ</sub>	—	1205	1197	26H <sub>ψ</sub> , 25H <sub>φ</sub> , 16K <sub>T</sub> , 14H <sub>γ</sub> , 14H <sub>θ</sub>
1150	1133	27H <sub>γ</sub> , 39 H <sub>θ</sub>	—	1150	1166	21H <sub>γ</sub> , 40H <sub>θ</sub> , 12K <sub>T</sub>
1107	1093	60K <sub>T</sub> , 10H <sub>θ</sub>	∧	1105	1089	49K <sub>T</sub> , 18H <sub>ξ</sub>
				1099	1083	43K <sub>T</sub> , 14H <sub>θ</sub> , 11H <sub>ξ</sub>

Table III (continued)

$\beta$ TPI				$\alpha$ TPI		
Freq (cm <sup>-1</sup> )		P.E.D. <sup>a</sup>		Freq (cm <sup>-1</sup> )		P.E.D. <sup>a</sup>
obs	calc	(%)		obs	calc	(%)
1058	1039	21K <sub>T</sub> , 25H <sub>ξ</sub>	—	1050	1051 1048	15K <sub>T</sub> , 38H <sub>ξ</sub> , 10H <sub>χ</sub> , 18H <sub>θ</sub> 20K <sub>T</sub> , 34H <sub>ξ</sub> , 18H <sub>θ</sub>
997	1010	33K <sub>T</sub> , 23H <sub>ξ</sub>	—	1030	1018	76K <sub>T</sub> , 24H <sub>ξ</sub> , -14F <sub>Tω</sub>
978	992	50H <sub>ξ</sub> , 16 K <sub>T</sub>	—	992	995 994	51H <sub>ξ</sub> , 26H <sub>θ</sub> 32H <sub>ξ</sub> , 26H <sub>θ</sub>
962	946	57H <sub>ξ</sub> , 25 K <sub>T</sub>	—	965	964 963	60H <sub>ξ</sub> , 19K <sub>T</sub> 56H <sub>ξ</sub> , 17K <sub>T</sub>
877	865	42Γ <sub>2</sub> , 24τ <sub>D</sub>	↙	882	886	41Γ <sub>2</sub> , 27τ <sub>D</sub>
			↘	862	872	49Γ <sub>2</sub> , 28τ <sub>D</sub>
800	816	55 K <sub>K</sub>	↙	800	816	20K <sub>K</sub> , 19K <sub>T</sub>
			↘	780	810	23K <sub>K</sub> , 20K <sub>T</sub>
750	742	51H <sub>χ</sub> , 21H <sub>θ</sub>	↙	750	770	24H <sub>χ</sub> , 30H <sub>θ</sub> , 12K <sub>T</sub>
			↘	730	750	51H <sub>χ</sub> , 19H <sub>θ</sub> , 10K <sub>T</sub>
600	586	26H <sub>β</sub> , 14H <sub>ε</sub> 20K <sub>T</sub>	↙	618	625	22H <sub>β</sub> , 29H <sub>ω</sub> , 19K <sub>K</sub>
			↘	555	573	27H <sub>β</sub> , 17H <sub>ω</sub> , 12K <sub>K</sub>

Table III (continued)

$\beta$ TPI			$\alpha$ TPI		
Freq (cm <sup>-1</sup> )		P.E.D. <sup>a</sup>	Freq (cm <sup>-1</sup> )		P.E.D. <sup>a</sup>
obs	calc	(%)	obs	calc	(%)
474	514	36 $\Gamma_1$ , 15 $\tau_D$	490	505	34 $\Gamma_1$ , 17 $\tau_D$ , 16 $H_\beta$ , 12 $H_\omega$
			470	490	36 $\Gamma_1$ , 19 $\tau_D$ , 15 $H_\beta$ , 12 $H_\omega$
--0	455	11 $H_\beta$ , 40 $H_\omega$ , 12 $K_T$	450	450	18 $\Gamma_1$ , 26 $H_\beta$ , 20 $H_\omega$ , 12 $K_T$
			441	441	17 $\Gamma_1$ , 11 $H_\epsilon$ , 32 $H_\omega$ , 10 $K_T$
	373	67 $H_\beta$ , 12 $K_T$	351	351	71 $H_\beta$ , 19 $H_\epsilon$
			316	316	78 $H_\beta$ , 16 $H_\epsilon$
	225	40 $H_\epsilon$ , 31 $H_\beta$	248	248	12 $H_\beta$ , 26 $H_\epsilon$ , 28 $H_\omega$
			233	233	15 $H_\beta$ , 22 $H_\epsilon$ , 17 $H_\omega$ , 10 $K_T$
	174	21 $\Gamma_1$ , 62 $H_\omega$	176	176	20 $H_\omega$ , 25 $H_\beta$ , 16 $\tau_D$
			150	150	10 $K_T$ , 25 $H_\beta$ , 16 $\tau_D$
	119	31 $\tau_R$	106	106	22 $H_\omega$ , 42 $\tau_R$
	90	40 $\tau_R$ , 23 $\tau_K$	91	91	46 $\tau_R$
	85	95 $\tau_K$	86	86	95 $\tau_K$
			81	81	96 $\tau_K$ gfh

<sup>a</sup> Contributions to potential energy distribution of >10%.

<sup>b</sup> Spectra not observed below 450 cm<sup>-1</sup> in this work.

crystalline spectra. For the beta form only one calculated frequency above  $450\text{ cm}^{-1}$  deviates from the observed value by more than  $20\text{ cm}^{-1}$ ; for the observed band at  $1280\text{ cm}^{-1}$  the deviation is  $42\text{ cm}^{-1}$ . One large deviation in calculated and observed bands occurs for alpha TPI; for the band observed at  $2879$  the deviation was  $35\text{ cm}^{-1}$ .

The calculated potential energy distribution, PED, shows that for the C-H stretching modes there is a unique assignment of one normal mode for each band. At lower frequencies mixed modes occur. The C=C stretch ( $K_D$ ), the  $\text{CH}_2$  scissoring, the  $\text{CH}_3$  asymmetric bend and the C-C stretch are the only modes that show more than a 60% contribution of a single normal coordinate to the potential energy distribution. All other modes show contributions of less than 60% for each calculated vibration.

Tentative band assignments are given in table IV. These assignments were made by considering the normal modes that contribute to each normal vibration in the molecule and by a comparison with assignments for other molecules containing similar chemical groups. Some normal vibrations

**Table IV**  
**Correlation of the observed crystalline and amorphous**  
**infrared frequencies<sup>a</sup>**

$\beta$ TPI observed frequency ( $\text{cm}^{-1}$ )	Amorphous TPI observed fre- quency ( $\text{cm}^{-1}$ )	$\alpha$ TPI observed frequency ( $\text{cm}^{-1}$ )	Type of vibration
3022 (sh) ———	3015 (sh) ———	3018 (sh)	$\nu_s(\text{=CH})$
2979 (sh) ———	2975 (sh) ———	2970 (s)	$\nu_{as}(\text{CH}_3)$
2965 (vs) ———	2961 (s) ———	2941 (vs)	$\nu_{as}(\text{CH}_3)$
2943 (vs) ———	2925 (vs) ———	2918 (vs)	$\nu_{as}(\text{CH}_2)$
2914 (vs) ———	2920 (vs) ———	2879 (vs)	$\nu_{as}(\text{CH}_2)$
2906 (vs) ———	2912 (vs) ———	2872 (vs)	$\nu_s(\text{CH}_3)$
2855 (s)		2855 (s)	
2846 (s) ———	2848 (s) ———	2830 (s)	$\nu_s(\text{CH}_2)$
1664 (m) ———	1665 (m) ———	1672 (m)	$\nu(\text{C=C})$
--	1570 (vw) ———	1574 (w)	
--	1540 (vw) ———	1541 (w)	
1450 (s) ———	1450 (s) ———	1450 (s)	$\delta(\text{CH}_2); \delta_{as}(\text{CH}_3)$
1430 (sh) ———	1430 (sh) ———	1430 (sh)	$\delta(\text{CH}_2)$
1384 (s) ———	1383 (s) ———	1380 (s)	$\delta_s(\text{CH}_3)$
	1360 (m) ———		
1348 (m) ———	1329 (m) ———	1340 (m)	$\alpha: \delta_s(\text{CH}_3) + \delta(\text{CH}_2)$ $\beta: \delta_s(\text{CH}_3) + \nu(\text{C-C})$
1324 (w) ———	1307 (sh) ———	1320 (w)	$\delta(\text{CH}_2)$
1280 (w) ———	1281 (w) ———	1280 (w)	$\delta(\text{CH}_2)$
1260 (m) ———	1253 (w-br) ———	1260 (w)	$\delta(\text{CH}_2)$
		1250 (w)	

$\beta$ TPI observed frequency (cm <sup>-1</sup> )	Amorphous TPI observed frequency (cm <sup>-1</sup> )	$\alpha$ TPI observed frequency (cm <sup>-1</sup> )	Type of vibration
1212 (m)	1220 (w)		
	1205 (w)	1205 (m)	$\delta(\text{=C-H})_{ip}$
1150 (m)	1150 (m)	1150 (m-w)	$\delta(\text{CH}_2)$
1107 (m)	1099 (m-s,br)	1105 (sh)	$\nu(\text{C-C})$
		1099 (m)	
1058 (vw)	1033 (m)	1051 (m)	$\delta_r(\text{CH}_3) + \nu(\text{C-C})$
997 (m)	987 (m)	1030 (m)	$\nu(\text{C-C}) + \delta_r(\text{CH}_3)$
978 (w)	976 (m)	996 (m)	$\delta_r(\text{CH}_3)$
962 (m)	924 (w)	965 (w)	$\delta_r(\text{CH}_3)$
	884 (sh)	882 (s)	
877 (s)	860 (sh)	862 (s)	$\delta(\text{=C-H})_{op}$
	842 (s)		
800 (s)	800 (sh)	800 (s)	$\nu(\text{C-CH}_3)$
		780 (sh)	
750 (m-s)	764 (m)	750 (w)	$\delta_r(\text{CH}_2)$
	743 (m)	734 (w)	
600 (ms)	595 (m)	618 (m)	$\delta(\text{C=C-C})$
-	570 (m)	555 (m)	
474 (s)	520 (m)	490 (m)	$\delta(\text{=C-CH}_3)_{op}$
	<505 (m)	470 (m)	

<sup>a</sup> s = strong; m = medium; w = weak; sh = shoulder.

<sup>b</sup>  $\nu$  = stretch;  $\delta$  = bend;  $\delta$  = twist, wag;  $\delta_r$  = rock.

are composed of a single normal mode and their assignment is therefore straight-forward. These include the stretching modes of  $\text{=C-H}$  ( $K_1$ ),  $\text{C=C}$  ( $K_D$ ),  $\text{C-C}$  ( $K_T$ ) and  $\text{C-CH}_3$  ( $K_K$ ), the asymmetric  $\text{CH}_3$  bending and  $\text{CH}_3$  rocking; and the bending of  $\text{C-C=C}$  ( $H_b$ ),  $\text{C=C-C}$  ( $H_e$ ), and of  $\text{C-C-C}$  ( $H_w$ ); as well as the different torsional modes.

Other vibrational mode assignments are composed of more than one normal mode and their assignment is therefore more complicated. For methyl and methylene stretching the symmetric and the asymmetric stretching modes were distinguished by assuming that the latter should be observed at a higher frequency (30-35). The methylene scissoring vibrations were assigned to bands whose PED included 80% HCH bending and 20% of the two HCC coordinates ( $\gamma$  and  $\theta$ ). It was not possible to distinguish equivocally between the twisting and the wagging methylene modes since they should both contain 50% contribution of each of the CCH coordinates and since they are both found in the same spectral region between 1250 and 1350 $\text{cm}^{-1}$ . The methylene group rocking is distinguishable from these modes

since its frequency is expected to be in the 730- 750  $\text{cm}^{-1}$  region (30-50). Finally, the out of plane bending modes of both the vinyl hydrogen and the vinyl methyl groups (44-47) were always coupled to the torsional coordinate of the double bond ( $t_D$ ).

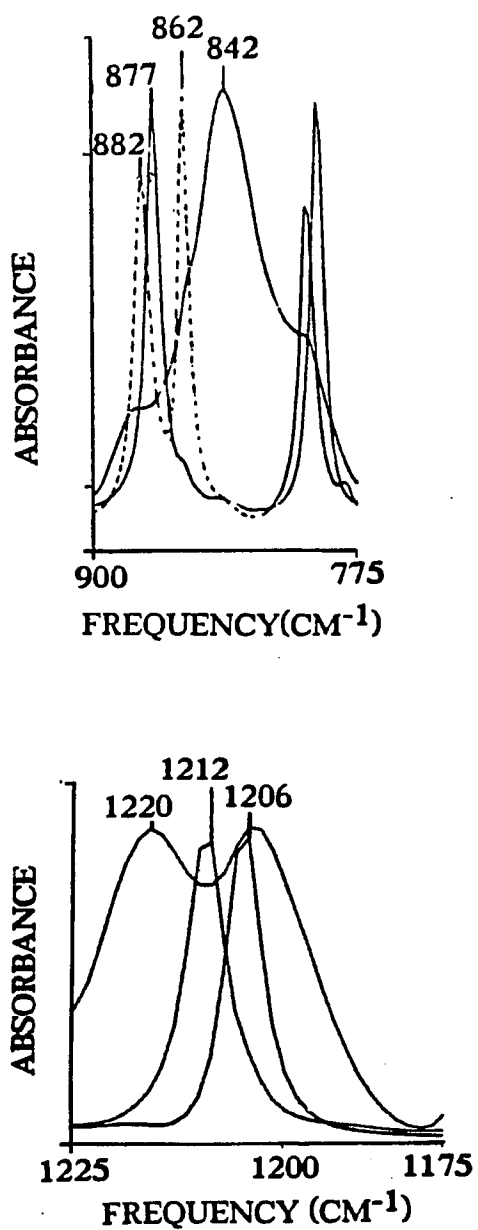
Comparison of the calculated PED for both crystal forms shows many differences between this work and the earlier study (24). For both crystal forms about half of these distributions differ in the two works. The principal discrepancies occur in the assignment for in-plane =C-H bending and for C-CH<sub>3</sub> stretching. The in plane =C-H bending mode was assigned previously at 1150  $\text{cm}^{-1}$  for both crystal forms; the present assignments at 1205  $\text{cm}^{-1}$  (alpha) and 1212  $\text{cm}^{-1}$  (beta) are in agreement with group frequency placement (13). The assignment of the band at 800  $\text{cm}^{-1}$  (alpha and beta) and at 780  $\text{cm}^{-1}$  (alpha) to C-CH<sub>3</sub> stretching is unique to the present work and arises from the introduction of a force constant characteristic of this particular bond. For the beta form the band at 1348  $\text{cm}^{-1}$  was previously assigned to methylene wagging and twisting

whereas in the present work it is found to be a mixed mode containing mainly methyl bending and some C-C stretching. For the beta form the amount of mode mixing reported in the two works varies for the bands at 1348, 1051, 997, 978 and 962  $\text{cm}^{-1}$ . In the 900 -1400  $\text{cm}^{-1}$  region for alpha TPI the earlier calculations show contributions of C-C stretching not found in the present work.

The frequencies of the maxima of the observed amorphous bands are listed in Table IV along with the crystalline assignments. These assignments were made by correlating the amorphous bands to crystalline ones and the transfer of the crystalline assignment. The correlation was obtained by overlaying each crystalline spectrum on the amorphous one. Each sharp crystalline band overlapped part of a broad amorphous band envelope although the maxima of the correlated bands were not the same in most cases. Examples for such band overlaps is shown in Figure 7. The correlation yields transfer of the same assignment from the alpha and beta crystalline spectra except for one case. The 1329  $\text{cm}^{-1}$  amorphous band is correlated to the crystalline

Figure 7 CORRELATION OF SPECTRAL BANDS

Overlap of correlated alpha and beta crystalline bands with amorphous trans-1,4 polyisoprene bands.



bands at 1348 and 1340 for beta and alpha TPI, respectively, which have different PED assignments.

#### ASSIGNMENT FOR AMORPHOUS BAND COMPONENTS

Amorphous spectra were obtained for the heated sample at intervals of 5°c between 65 and 110°C. Two of these spectra which were obtained between 700-1300cm<sup>-1</sup> are given in Figure 8 for the 65 and 110°c samples. Heating of the partially crystalline sample above 65°c resulted in the loss of all the sharp crystalline peaks. At higher temperatures a decrease in band intensities was observed as well as changes in the contours of some of the broad amorphous bands. The detailed changes taking place upon heating TPI above the melting temperature can be best followed by using difference spectra, two of which are given in Figure 9 . The difference spectra were obtained by subtracting each of the spectra taken at different temperatures from the 110°c spectrum. The changes that occur in the spectrum with temperature were followed by observing the minima in the difference spectra which do not

**Figure 8**      SPECTRA OF TPI AT HIGH TEMPERATURES

Infrared spectra of amorphous trans-1,4 polyisoprene at temperatures above the melting point.

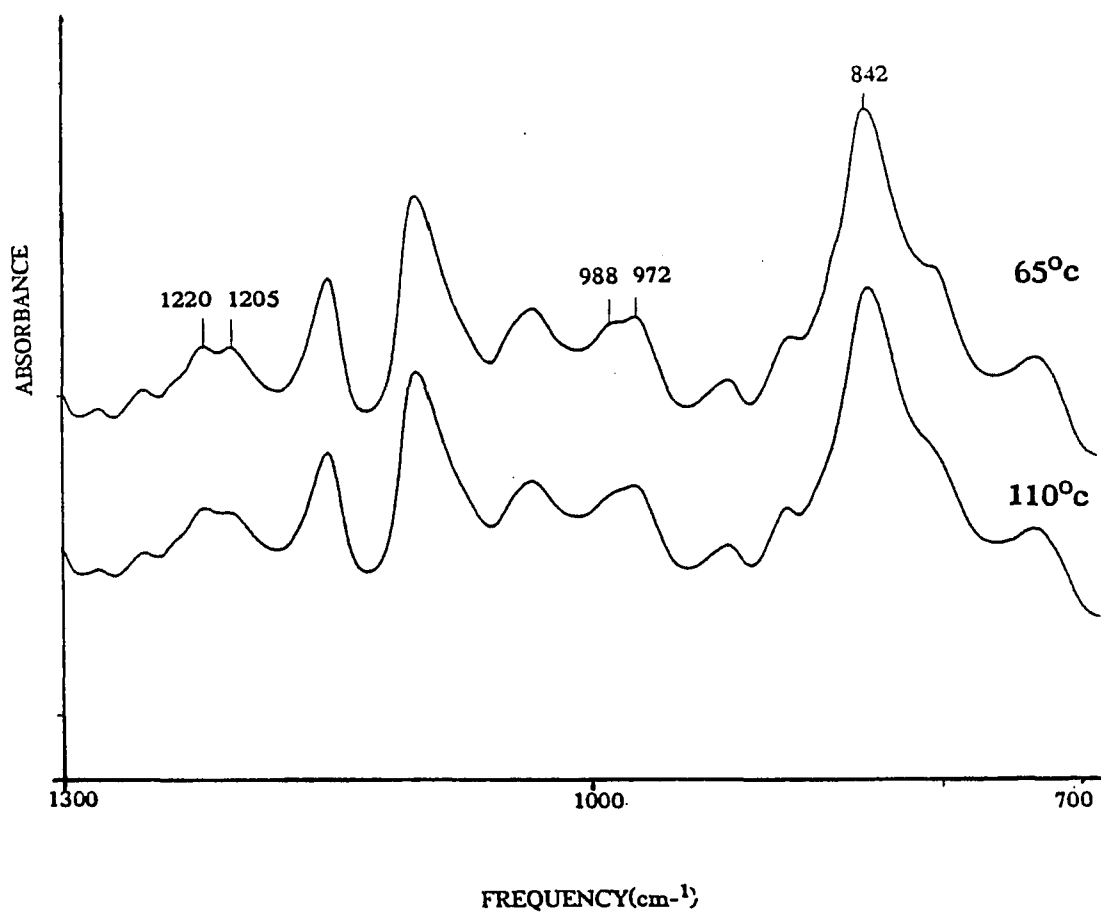
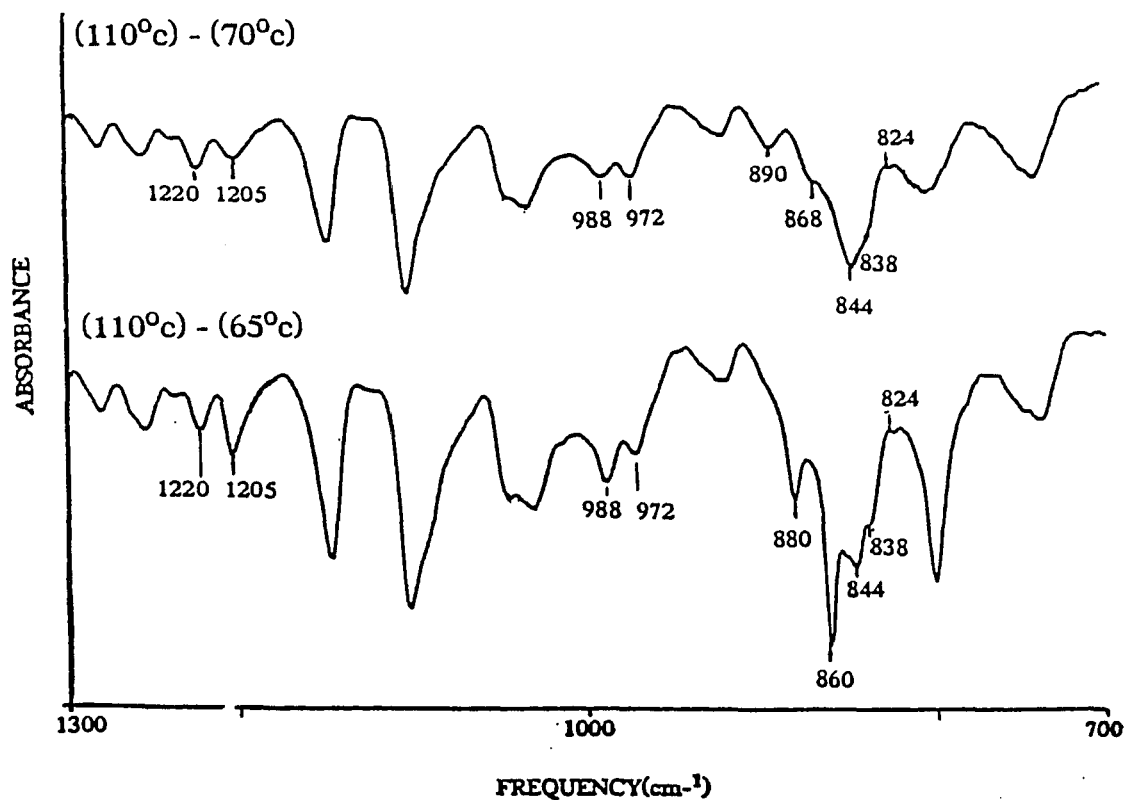


**Figure 9**      CHANGES IN TPI SPECTRA AT HIGH TEMPERATURES

Difference spectra of amorphous trans-1,4 polyisoprene. A) Subtraction of a spectrum obtained at 70°C from a spectrum obtained at 110°C.

B) Subtraction of a spectrum obtained at 65°C from a spectrum obtained at 110°C.



all correspond to maxima in amorphous bands but take place within the complex band contour. The use of different reference spectra in the subtraction shows that some of these changes are not gradual but occur just above  $T_m$ . The components of conformationally sensitive bands at 800-810, 824-890, 970-985, 1100-1105 and 1200-1235  $\text{cm}^{-1}$  are listed and identified in Table V. The conformational assignments given in this table will be discussed below in more detail. The changes that were observed in the spectrum between 70 and 110°C are gradual and continue to occur throughout this temperature range.

#### SURFACE MODIFICATION

The reaction of TPI lamellas in suspension resulted in the partial modification of the TPI chain. The lamellar surface was reacted while the crystalline core remained unchanged forming segmented block copolymers with alternating sequences of TPI and of modified TPI units. This product had been previously characterized by  $^1\text{H}$  NMR and by  $^{13}\text{C}$  NMR.

The reaction with m-chloroperbenzoic acid leads to the

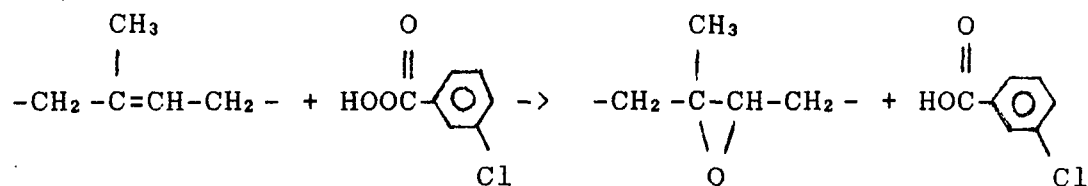
**Table V Infrared Frequencies and Band Component Assignments  
for *trans*-1,4-Polyisoprene in the Melt**

Absorbance Spectra Frequencies-cm <sup>-1</sup>	Difference Spectra Ref. Temp. 65°C	Frequencies-cm <sup>-1</sup> Ref. Temp. 70°C	Conformational Assignment
800	800	800	trans
	-	808	gauche
840*	824	824	cis/gauche
	838	838*	gauche
	844	844	gauche
	860	862*	-
	867	-	868
	882	-	trans
	-	890	trans
972*	972	972	gauche
	984	988*	trans
1099	1090	1090	gauche
	1105*	1105*	trans
1204	1204*	1202	trans
	1220	1220*	gauche
	1235	1235	

\* denotes largest component of a band

Difference spectra were obtained by subtracting the spectrum taken at the reference temperature from the spectrum taken at 110°C.

epoxidation of the surface double bonds as follows:



The FTIR spectra of surface epoxidized TPI is shown in Figure 10 for lamellas with alpha and beta crystal forms. The separate spectrum of the epoxidized surface itself is shown in Figure 12a. It was obtained by subtraction of the crystalline TPI spectrum with the appropriate form from the spectra in Figure 11.

The surface epoxidized spectra (Figure 12a) differs from the amorphous TPI spectrum (Figure 12b) mainly in the following respects: i) the 1665 band, the 595/570 doublet and the 520/490  $\text{cm}^{-1}$  doublet disappear; ii) new bands appeared at 1250, 1122, 1069, 685 and 540  $\text{cm}^{-1}$ ; and, iii)

The band at 842 is replaced by one at 880  $\text{cm}^{-1}$ .

Hydrochlorination of TPI lamellar structure in suspension proceeds by Markownikoff addition (8):

Infrared spectra of surface epoxidized trans-1,4 polyisoprene lamellas. A) With a crystal core of the alpha form. B) With a crystal core of the beta form.

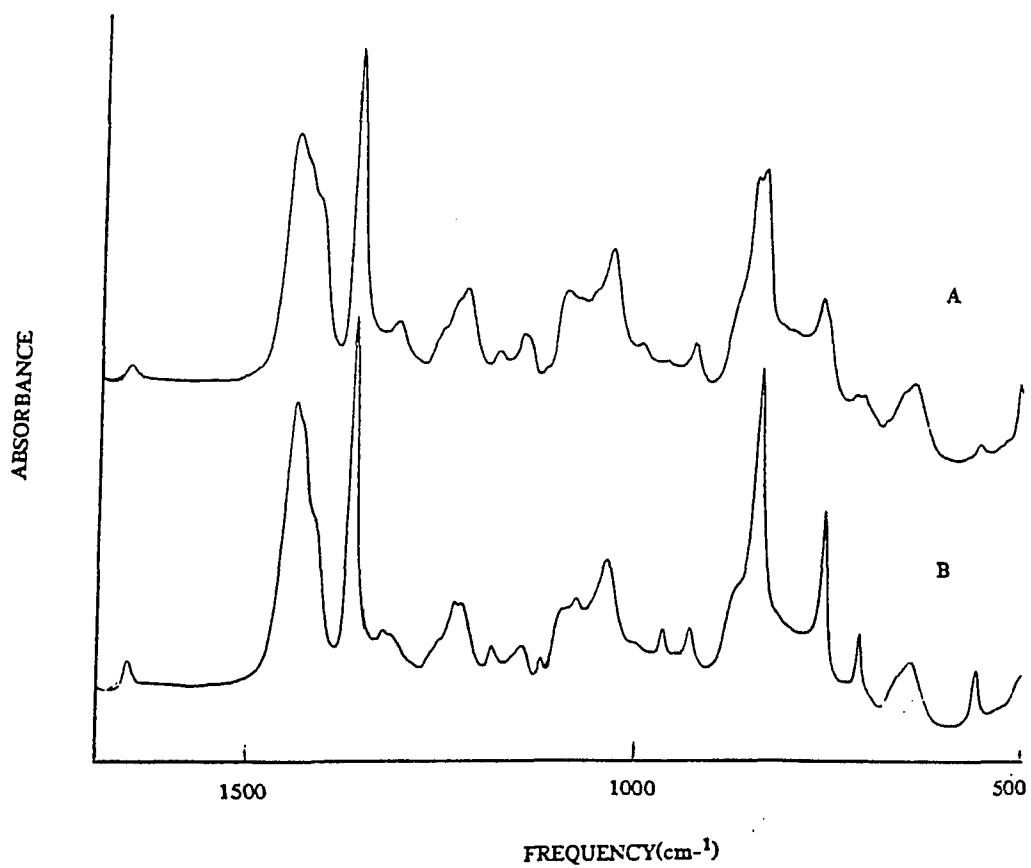
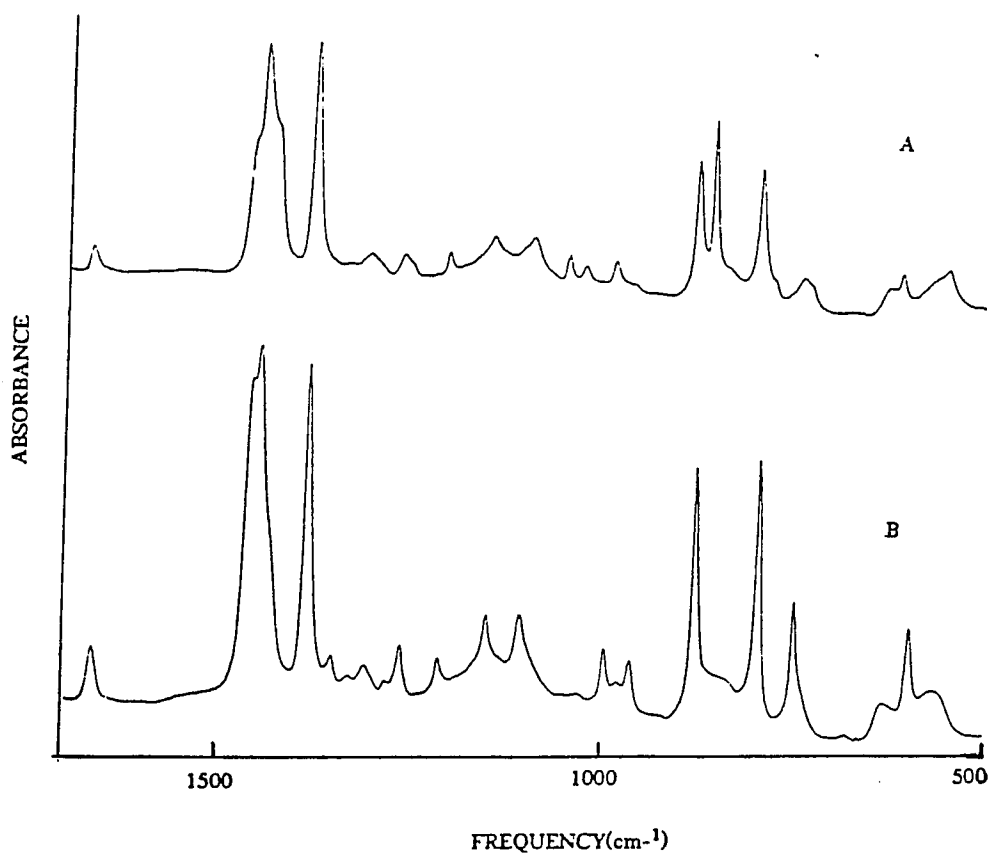


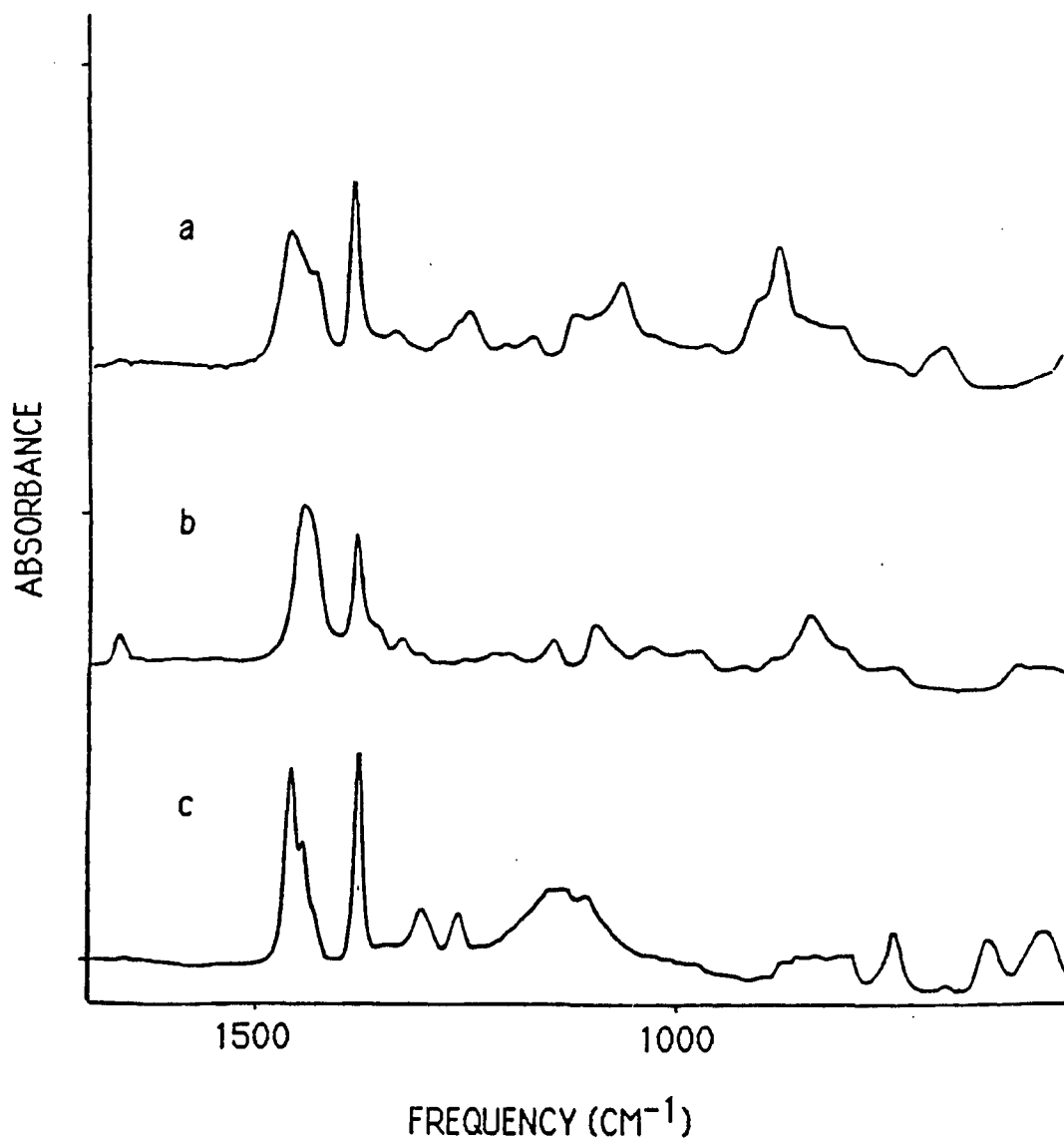
Figure 11 SPECTRUM OF HYDROCHLORINATED TPI

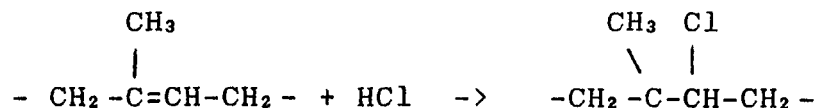
Infrared spectra of trans-1,4 polyisoprene lamellas with hydrochlorinated surfaces. A) With a crystal core of the alpha form. B) With a crystal core of the beta form.



**Figure 12**      SPECTRA OF MODIFIED TPI LAMELLAR SURFACE

Infrared spectra of modified trans-1,4 polyisoprene lamellar surface. A) Epoxidized. B) Unmodified. C) Hydrochlorinated.





The FTIR spectra of two partially hydrochlorinated samples with alpha and beta crystal forms are shown in Figure 11 a and b respectively. Subtraction of the appropriate crystalline component yields the spectrum of the hydrochlorinated surface itself which is shown in figure 12c. Comparison of this spectrum with that of the unmodified amorphous TPI shows: i) The absence of bands at 1664, 842, 595 and 520-490  $\text{cm}^{-1}$ ; ii) the presence of new bands at 1140, 684, 635 and 565  $\text{cm}^{-1}$ ; and, iii) an increase in intensity of the bands at 1306, 1261, 1155 and 746  $\text{cm}^{-1}$ . Tentative band assignments for the modified amorphous TPI were made by correlation and transfer from amorphous TPI bands; these are given in Table VI.

Hydroxylation of TPI lamellar surface was done in two steps. In the first step the double bond is esterified by osmium tetroxide in suspension in amyl acetate:

**Table VI**  
**Infrared Frequencies and Band Assignments for Amorphous,**  
**Epoxidized, and Hydrochlorinated TPI<sup>a</sup>**

EP TPI	TPI	Cl TPI	Assignment <sup>b</sup>
--	3025 (w)	--	$\nu(\text{C-H})$
3022 (w)	--	--	$\nu(\text{-C-H})$
2991 (s) _____	2976 (s) _____	2983 (s)	$\nu_{\text{as}}(\text{CH}_3)$
2964 (vs) _____	2961 (vs) _____	2957 (vs)	
2932 (vs) _____	2934 (vs) _____	2933 (vs)	$\nu_{\text{as}}(\text{CH}_2)$
2926 (vs) _____	2920 (vs) _____	2928 (vs)	
2914 (s) _____	2912 (s) _____	2912 (s)	$\nu_{\text{s}}(\text{CH}_3)$
2875 (s) _____	2875 (s) _____	2873 (s)	$\nu_{\text{s}}(\text{CH}_2)$
2858 (s) _____	2848 (s) _____	2842 (s)	
--	1668 (m)	--	$\nu(\text{C=C})$
--	1574 (vw)	--	--
--	1541 (vw)	--	--
1462 (s) _____	1450 (s) _____	1460 (s)	$\delta(\text{CH}_2); \delta_{\text{as}}(\text{CH}_3)$
1433 (sh) _____	1430 (sh) _____	1446 (sh)	$\delta(\text{CH}_2)$

Table VI (continued)

EP TPI	TPI	CI TPI	Assignment <sup>b</sup>
1387 (s)	1380 (s)	1383 (s)	$\delta_s(\text{CH}_3)$
	1360 (sh)		
1336 (w)	1329 (m)	1344 (w)	$\delta_s(\text{CH}_3)+\nu(\text{C}-\text{C})$ $\delta_s(\text{CH}_3)+\delta(\text{CH}_2)$
1312 (sh)	1307 (sh)	1305 (m)	$\delta(\text{CH}_2)$
1280 (sh)	1281 (w)		$\delta(\text{CH}_2)$
1260 (sh)	1253 (w)	1261 (m)	$\delta(\text{CH}_2)$
1250 (ms)	--	--	$\nu_s(\text{EP})$
--	--	1234 (vw)	--
--	1220 (w)	--	$\delta(=\text{CH})_{\text{ip}}$
--	1205 (w)	--	
1208 (w)	--	--	--
1174 (m)	1150 (m)	1155 (m-s)	$\delta(\text{CH}_2)$
		1140 (m-s)	
1122 (m-s)	--	--	$\nu_{\text{as}}(\text{EP})$

Table VI (continued)

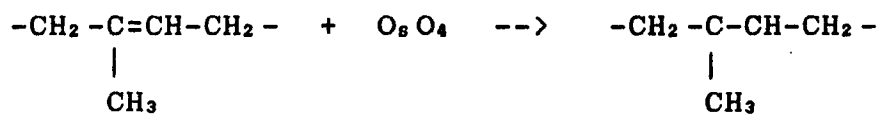
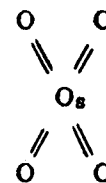
EP TPI	TPI	CI TPI	Assignment <sup>b</sup>
1099 (sh) _____	1099 (m-s) _____	1110 (m-s)	$\nu(\text{C-C})$
1069 (s)	--	--	$\nu_{\text{as}}(\text{EP})$
1032 (sh) _____	1033 (m) _____	1031 (sh)	$\delta_{\text{r}}(\text{CH}_3) + \nu(\text{C-C})$
1010 (sh) _____	987 (m) _____	1010 (sh)	$\delta_{\text{r}}(\text{CH}_3) + \nu(\text{C-C})$
990 (sh) _____	976 (m) _____	976 (sh)	$\delta_{\text{r}}(\text{CH}_3)$
965 (w) _____	924 (w) _____	950 (w)	$\delta_{\text{r}}(\text{CH}_3)$
900 (sh)			
880 (s)	--	--	$\delta(\text{-C-H})_{\text{op}}$
853 (sh)			
	884 (sh)		
--	862 (sh)	--	$\delta(\text{=C-H})_{\text{op}}$
	842 (s)		
--	--	876 (w)	--
--	--	855 (w)	--
--	--	837 (w)	--
800 (m) _____	800 (m) _____	804 (w)	$\nu(\text{C-CH}_3)$

Table VI (continued)

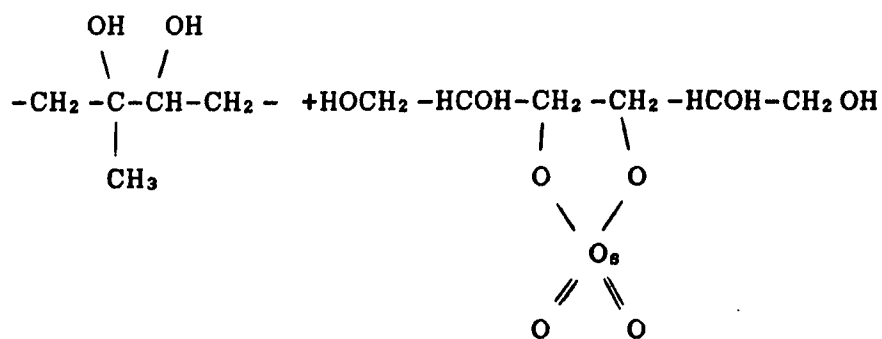
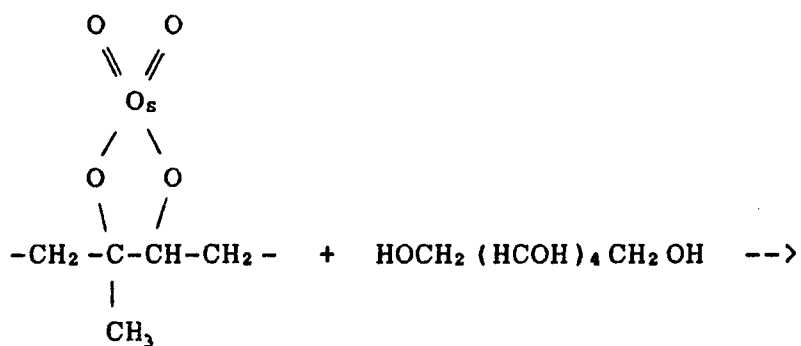
EP TPI	TPI	Cl TPI	Assignment <sup>b</sup>
765 (sh) ———	764 (sh)	746 (m-s)	$\delta_r(\text{CH}_2)$
746 (m) ———	746 (m)		
700 (sh)			
685 (m-s)	--	--	$\delta(\text{EP})$
--	--	684 (w)	--
--	--	635 (m)	$\nu(\text{C-Cl})$
--	595 (m)	--	$\delta(\text{C=C-C})$
--	570 (m)	--	
--	--	565 (m-s)	$\nu(\text{C-Cl})$
540 (m)	--	--	$\delta(-\text{C-CH}_3)_{\text{op}}$
--	520 (m)	--	$\delta(=\text{CCH}_3)_{\text{op}}$
	<505 (m)		

<sup>a</sup> EP=epoxidized, Cl=hydrochlorinated, s = strong, m = medium, w = weak, sh = shoulder.

<sup>b</sup>  $\nu$  = stretch;  $\delta$  = bend;  $\delta_r$  = twist, wag;  $\delta_r$  = rock; EP = epoxy ring.



In a second step a transesterification takes place when the polymer is in methylene chloride solution:



The osmium addition is fast and expected to be quantitative without side reactions (96,97). It takes place in amyl acetate where the osmium tetroxide is extremely soluble. The second step is more complex. Since hydroxylation is extremely slow in suspension (98), the polymer was dissolved in methylene chloride. The mannitol, which is the transesterification reagent (99-102), was in a basic water solution so that the reaction took place in the water/methylene chloride interface. These conditions slowed the reaction down considerably. Most of the polymer reacted within a few hours, as evident by the change in color from the black osmate to the white diol. However, some gray spots remained on the polymer and disappeared only after 30 days. The reaction process was also evident by the fact that the polymer came out of solution and precipitated at the water/methylene chloride interface.

The spectrum of the partially hydroxylated sample is shown in Figure 13a. Subtractions of the appropriate crystalline form and of the amorphous TPI spectrum yield the spectrum of the hydroxylated surface which is shown in

Figure 13 SPECTRUM OF HYDROXYLATED TPI

Infrared spectra of trans-1,4 polyisoprene. A) Partially hydroxylated. B) Hydroxylated.

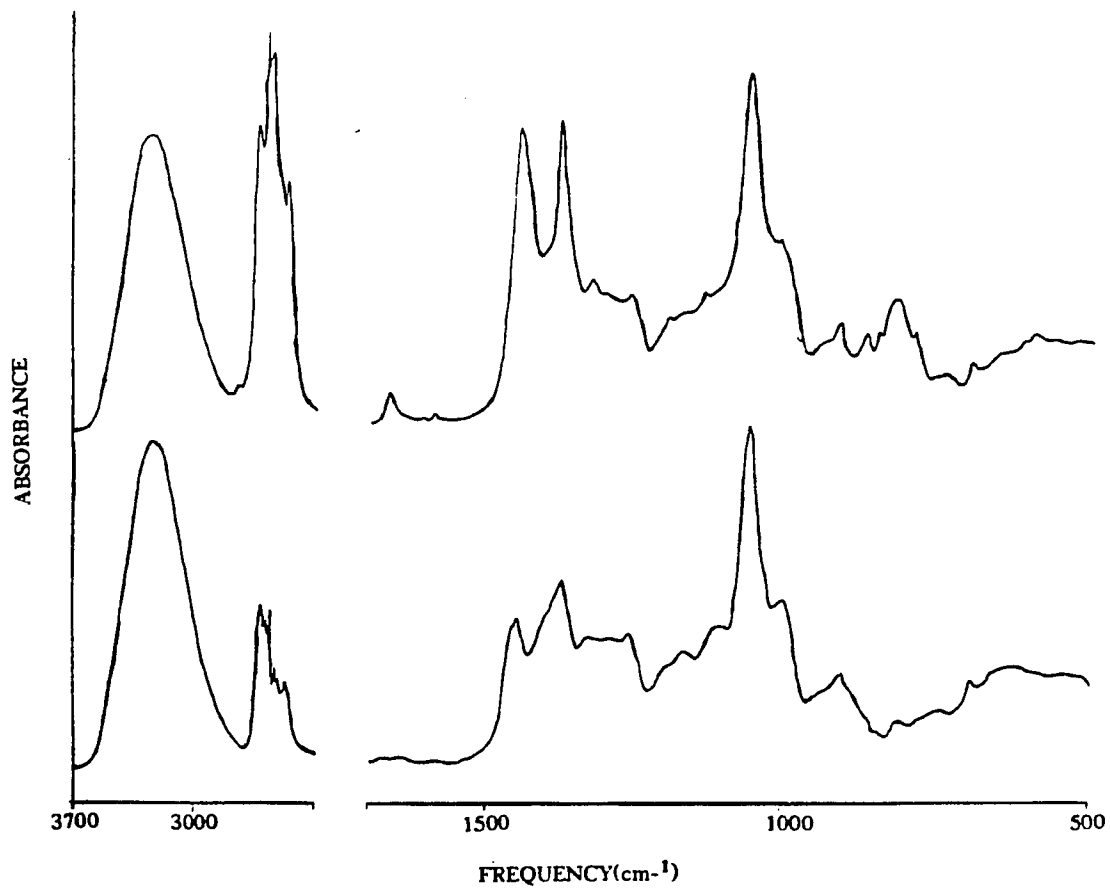


Figure 13b. The frequency of the vibrational modes of hydroxylated TPI are given in Table VII. Comparison of this spectrum with that of unmodified amorphous TPI shows: i) the absence of bands at 1664 and 842. ii) the presence of new bands at 3400, 1390, 1074, 1026, 931 and 710  $\text{cm}^{-1}$ . Tentative assignment for the hydroxylated TPI bands were made by correlation and transfer from amorphous TPI bands; these are given in table VII.

The NMR spectrum of the product has not been obtained because of its low solubility in most solvents. Solubility tests were done for the copolymer product using many solvents such as alcohols, haloalkanes, ethers, DMSO, DMF and THF. The product was insoluble in all of them. The only two liquids that showed some solubility were pyridine and hexanoic acid. These solvents were chosen since they contain a polar and a non-polar part which are needed to dissolve the copolymer structure. Pyridine did not dissolve the polymer completely even at higher temperatures. The NMR spectrum of the product in pyridine showed only the

Table VII

wave number (cm <sup>-1</sup> )	Assignments <sup>a</sup>
3040	(O-H) st
1450	(CH <sub>2</sub> ) bend, (CH <sub>3</sub> ) as bend
1390	(COH) bend
1383	(CH <sub>3</sub> ) bend
1334	(CH <sub>3</sub> ) bend, (CH <sub>2</sub> ) w+t
1300	(CH <sub>2</sub> ) w+t
1265	(CH <sub>2</sub> ) w+t
1177	-
1074	(C-O) st
1026	(C-O) st
931	-
830	-
763	(CH <sub>2</sub> ) r
742	(CH <sub>2</sub> ) r
710	-

a) st=stretching, as= asymmetric, s= symmetric,  
w= wagging, t= twisting, r= rocking.

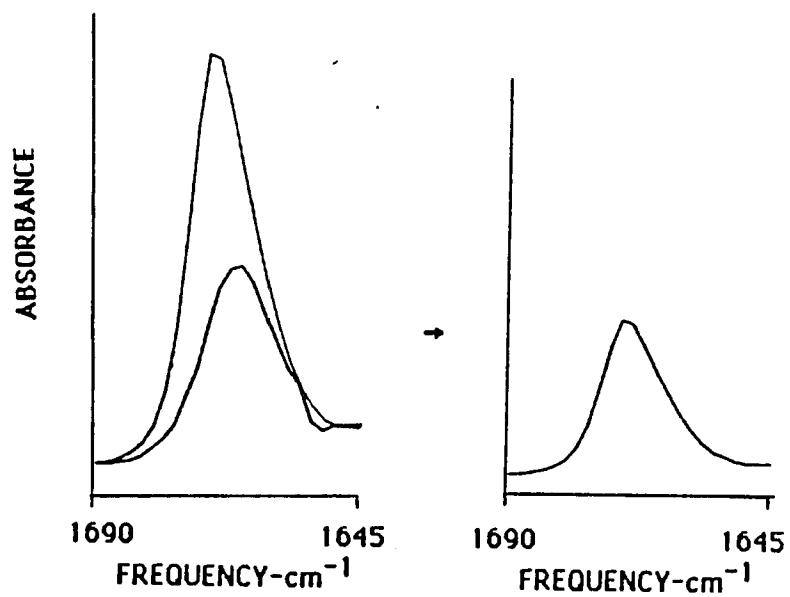
unreacted TPI segments. The copolymer seemed to be completely soluble in the hexanoic acid. However, the spectrum was unclear since the copolymer resonance peaks were completely obscured by the many large solvent peaks.

#### CRYSTALLINITY MEASUREMENTS

A procedure for a direct measurement of sample crystallinity from infrared spectra was developed. A semicrystalline spectrum was obtained for the measured sample at ambient temperature. This spectrum was used to obtain the 100% crystalline spectrum by subtraction of the amorphous spectrum obtained at 65°C. This subtraction was carried out by watching the disappearance of the 842  $\text{cm}^{-1}$  band until negative components appeared throughout the spectrum. The crystallinity is then calculated from the relative areas of the 1664-72  $\text{cm}^{-1}$  band before and after the subtraction. This procedure is illustrated in Figure 14, which shows on the left-hand side a semicrystalline band envelop ranging from 1690 to 1645  $\text{cm}^{-1}$  and the scaled amorphous band at the same region which is subtracted from

Figure 14 DIGITAL SUBTRACTION OF TPI SPECTRA

Spectral subtraction in the 1645-1690  $\text{cm}^{-1}$  region used to obtain the crystalline component of the trans-1,4 polyisoprene band.



it; the difference between these two bands which is the 100% crystalline component is shown on the right-hand-side. This procedure was used for five types of TPI samples with different morphologies and/or crystal forms.

Crystallinity measurements from density were also obtained for some of the above samples. The sample density was measured using a gradient column whose density changes linearly with the column height. The linearity of the column was calibrated with precalibrated glass beads. The crystallinity data for the various samples are summarized in Table VIII.

Infrared and density measurements of samples crystallinity were performed on mats of TPI lamellas subjected to a pressure of 200 psi. Application of 200 psi, the smallest pressure used, caused an average decrease in 6% in the sample crystallinity. These results are included in Table VIII. Higher pressures up to 2000 psi did not bring about further change in crystallinity.

Infrared crystallinities at different temperatures were

**Table VIII**  
**Crystallinity of TPI Samples from Solution**

sample	solvent	T <sub>c</sub> , °C	crystal form	% crystallinity	
				IR	density
Synthetic 1	AA	0/30	β	63	62
2				65	63
3				65	64
4				63	--
Synthetic (pressed 1)				57	--
Balata 1				61	--
2				61	61
3				59	61
4				60	--
Gutta Percha 1				60	60
2				60	--
3				59	58
Synthetic 5		30	α	54	--
6				56	--
7				55	--
Synthetic (pressed 2)				50	--

Synthetic 8	hexane	20	$\alpha$	56	--
9				54	--
10				55	--

measured on semicrystalline TPI samples with alpha and beta crystalline cores. FTIR spectra were obtained in a heating experiment for the sample from ambient temperature up to 110°C at intervals of five degrees. Samples prepared in the same way were cooled down to -145°C and spectra were obtained at intervals of about ten degrees. The results of the infrared measurements at different temperatures are shown in Figure 15. The crystallinity gradually increases with a temperature decrease down to -30°C and then levels off. The total increase in crystallinity between room temperature and -30°C is 10%. Above ambient temperatures the crystallinity gradually decreases until about 40°C above which a sharp decrease occurs in the crystallinity.

#### TPI SPECTRA AT LOW TEMPERATURE

Infrared spectra taken in the 700 to 1700  $\text{cm}^{-1}$  region at ambient temperature and at -145°C for semicrystalline TPI with crystalline core of the alpha form which was prepared by direct cooling (sample #2) are shown in Figure 16. Spectra obtained at the same two temperatures with a

Figure 15 CRYSTALLINITY MEASUREMENTS

The changes in percent crystallinity of trans-1,4 polyisoprene lamellas with temperature.

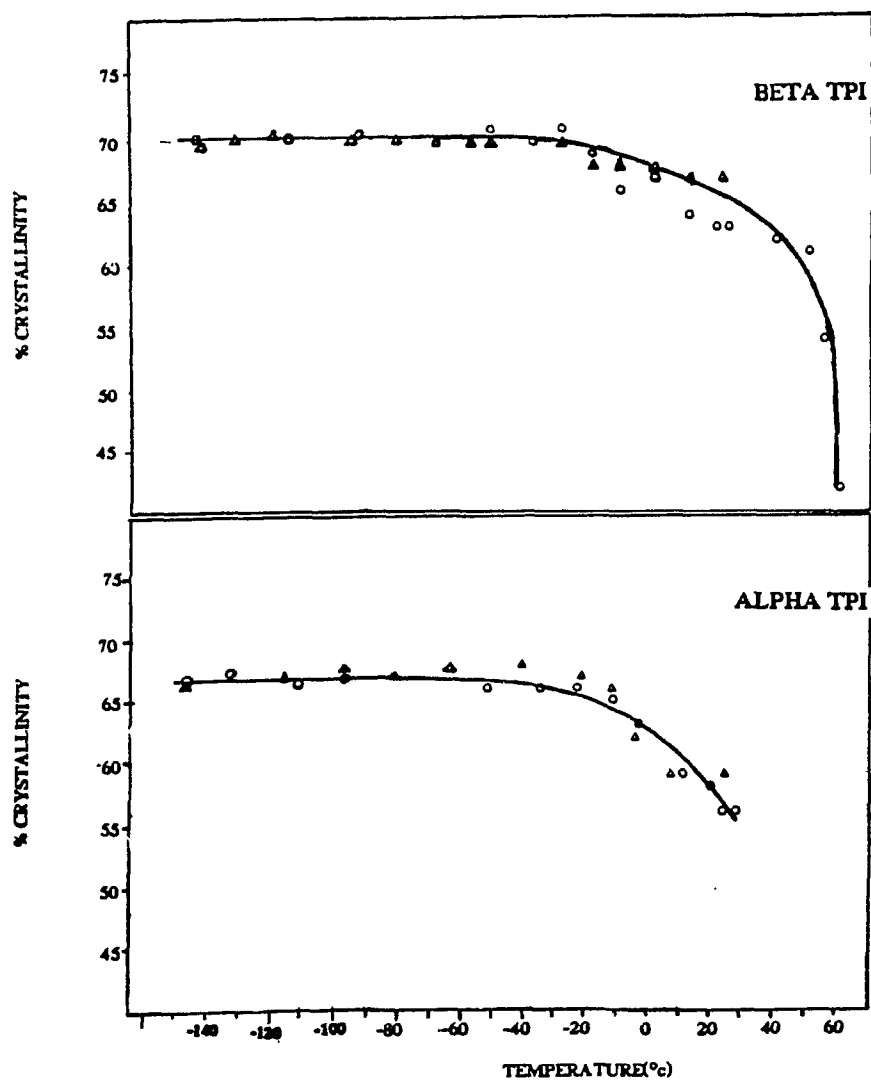
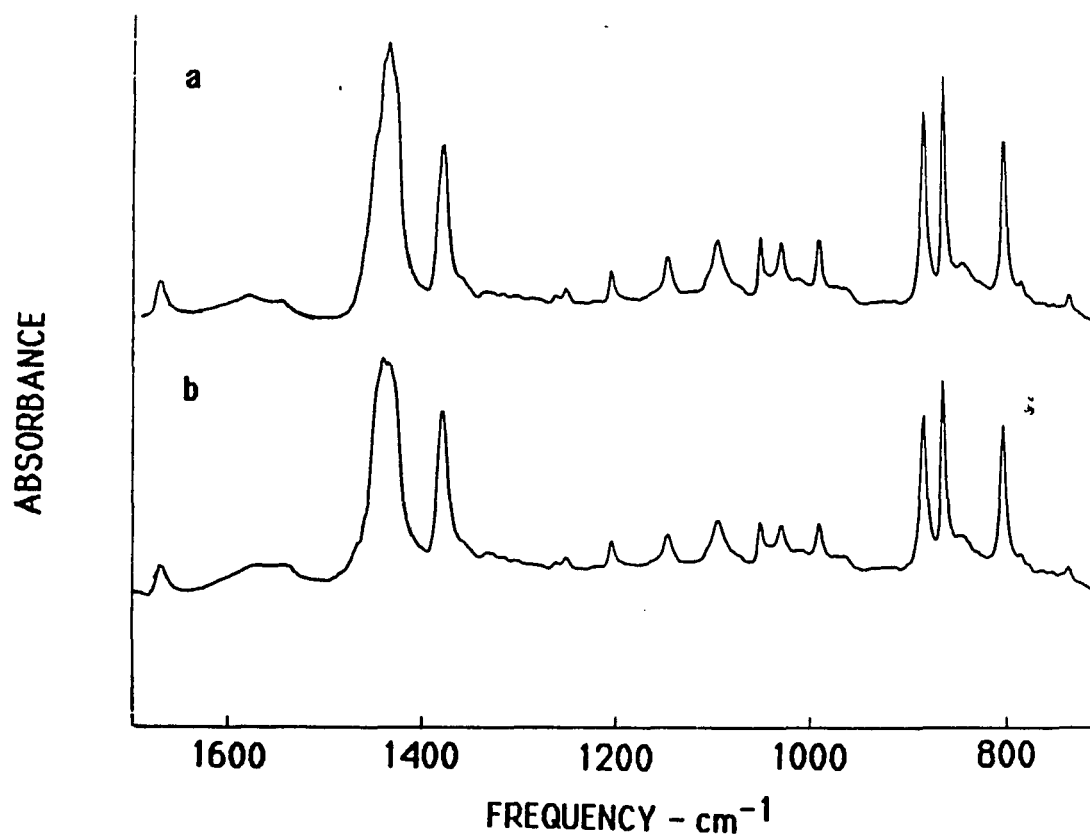


**Figure 16**      ALPHA TPI SPECTRUM AT LOW TEMPERATURES

Infrared spectra in the 700-1700  $\text{cm}^{-1}$  region of trans-1,4 polyisoprene lamellas containing the alpha crystal form.

A) at  $-145^{\circ}\text{C}$ . B) at room temperature.



beta form crystalline core are given in Figure 17. For samples with either crystal form many of the bands show an increase in intensity with decreasing temperature. The low temperature spectrum for the beta TPI sample shows splitting of the  $1447\text{ cm}^{-1}$  band into a shoulder at  $1462\text{ cm}^{-1}$  and a doublet at  $1439/1447\text{ cm}^{-1}$ . In addition the same sample shows nonsymmetrical narrowing of  $11\text{ cm}^{-1}$  for the band at  $1105\text{ cm}^{-1}$  and of  $3\text{ cm}^{-1}$  for the bands at  $997$ ,  $978$  and  $962\text{ cm}^{-1}$  and a frequency shift of  $+4\text{ cm}^{-1}$  for the  $877\text{ cm}^{-1}$  band. For the sample with an alpha crystalline core a narrowing occurs at  $1030\text{ cm}^{-1}$  by  $3\text{ cm}^{-1}$ .

The changes in the spectrum of a particular sample that occur at low temperature are best seen when difference spectra are used. Difference spectra for semicrystalline samples containing either the alpha or the beta crystalline form, obtained by subtraction of the room temperature spectrum separately from each spectrum taken at low temperatures, are shown in Figures 18 and 19. The difference spectra show positive bands at frequencies which are associated with vibrational frequencies of the

**Figure 17**      BETA TPI SPECTRUM AT LOW TEMPERATURES

Infrared spectra in the 700-1700  $\text{cm}^{-1}$  region of trans-1,4 polyisoprene lamellas containing the beta crystal. A) at  $-145^{\circ}\text{C}$ . B) at room temperature.

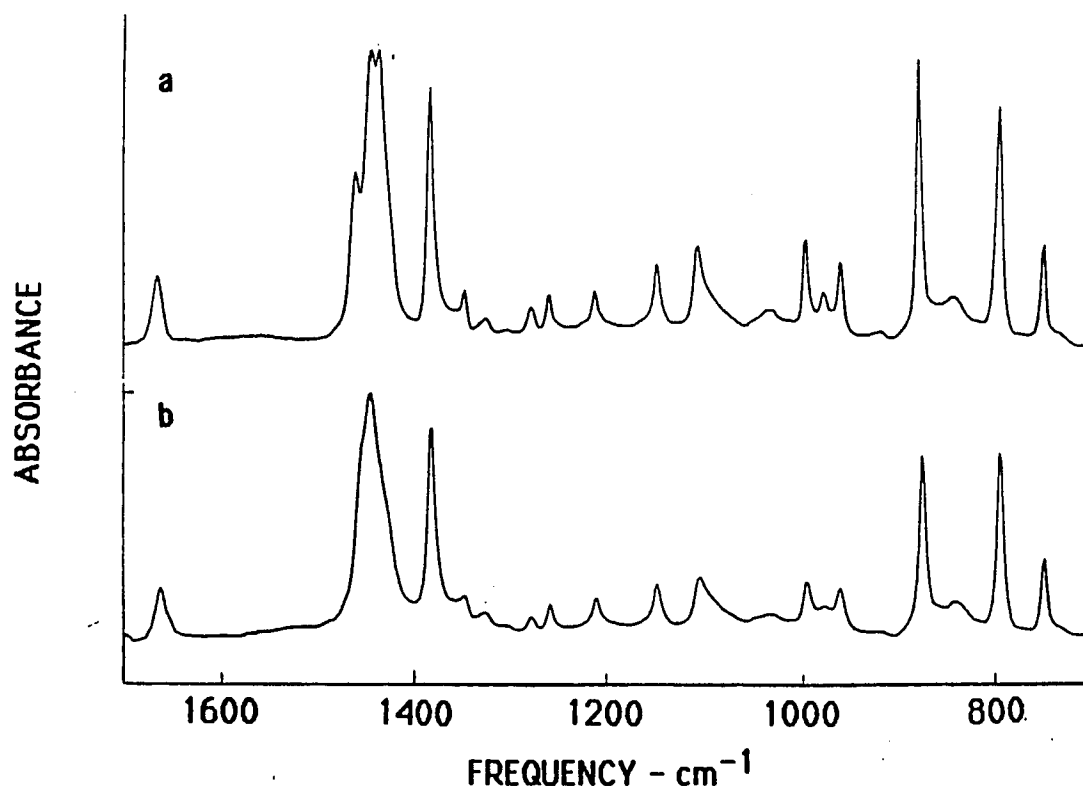
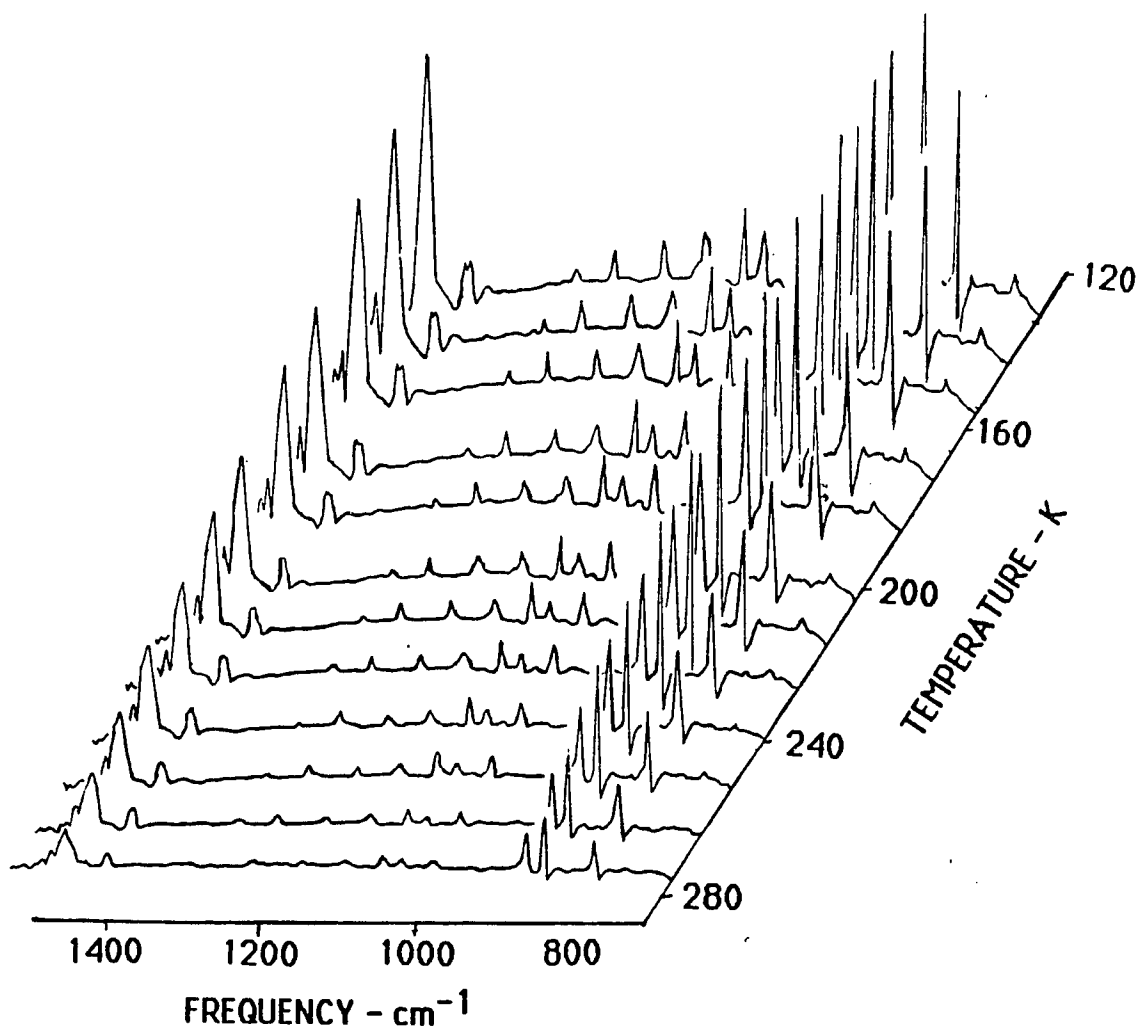


Figure 18 CHANGES IN ALPHA TPI SPECTRUM

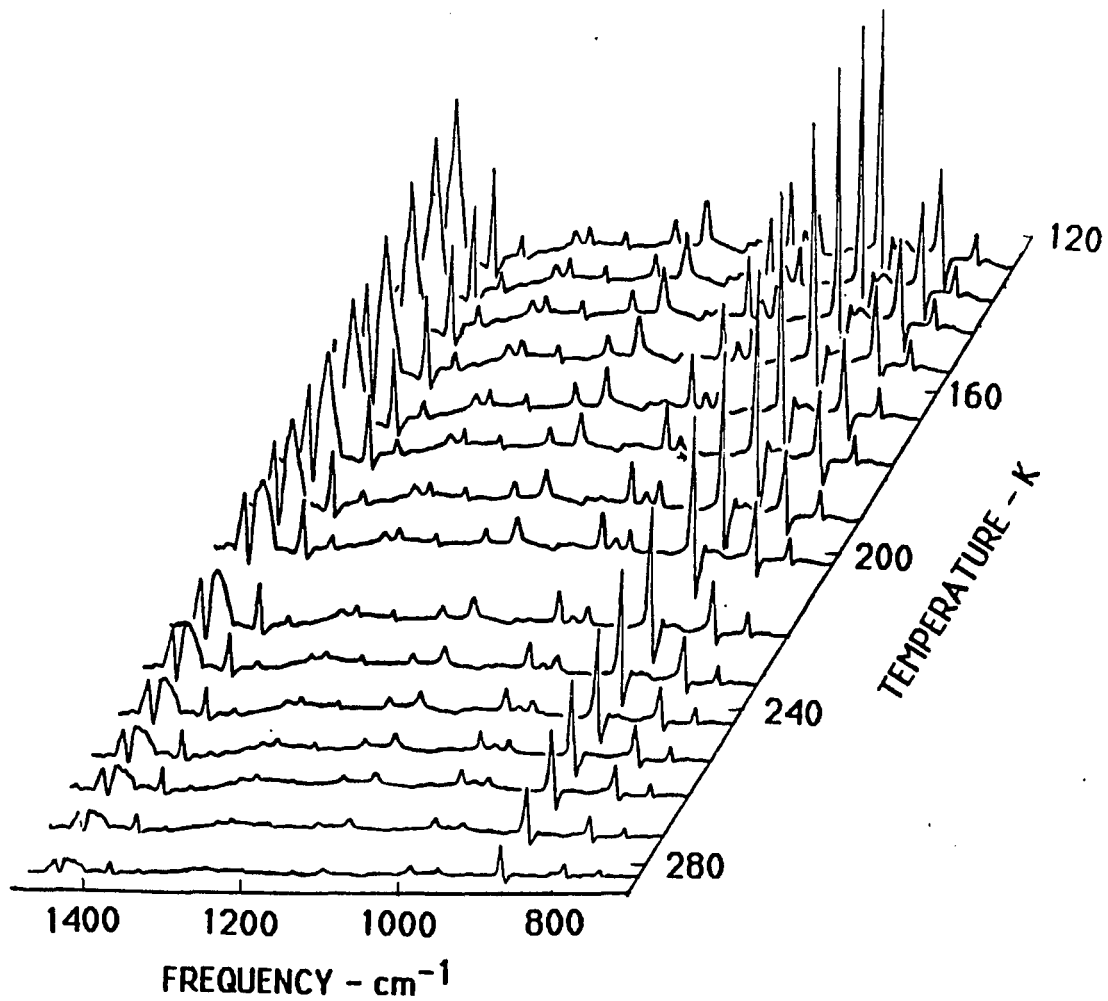
AT LOW TEMPERATURES

Difference spectra from 700 to 1700  $\text{cm}^{-1}$  region for trans-1,4 polyisoprene lamellas containing the alpha crystal form. Subtraction of a room temperature spectrum from a spectrum recorded at temperature T.



**Figure 19**      CHANGES IN BETA TPI SPECTRAAT LOW TEMPERATURES

Difference spectra from 700 to 1700  $\text{cm}^{-1}$  for trans-1,4 polyisoprene lamellas containing the beta crystal form. Subtraction of a room temperature spectrum from a spectrum recorded at temperature T.



crystalline form that exists in each sample. Negative components appear adjacent to some of these positive bands. The negative/positive changes are caused by the frequency shift of the band or by its non-symmetrical narrowing. A symmetrical band narrowing would have appeared in the difference spectra as a negative/positive/negative effect. In the beta spectrum the bands that show the negative components are the asymmetric and the symmetric bending modes of the methyl group at 1462 and at 1385  $\text{cm}^{-1}$ , the =C-H in- and out-of-the-plane bending modes at 1212 and at 877  $\text{cm}^{-1}$  and the C-CH<sub>3</sub> stretching mode at 800  $\text{cm}^{-1}$ . For the alpha spectrum only the alpha doublet due to the =C-H out of the plane bending and the C-CH<sub>3</sub> stretching show a negative/positive effect in the difference spectra.

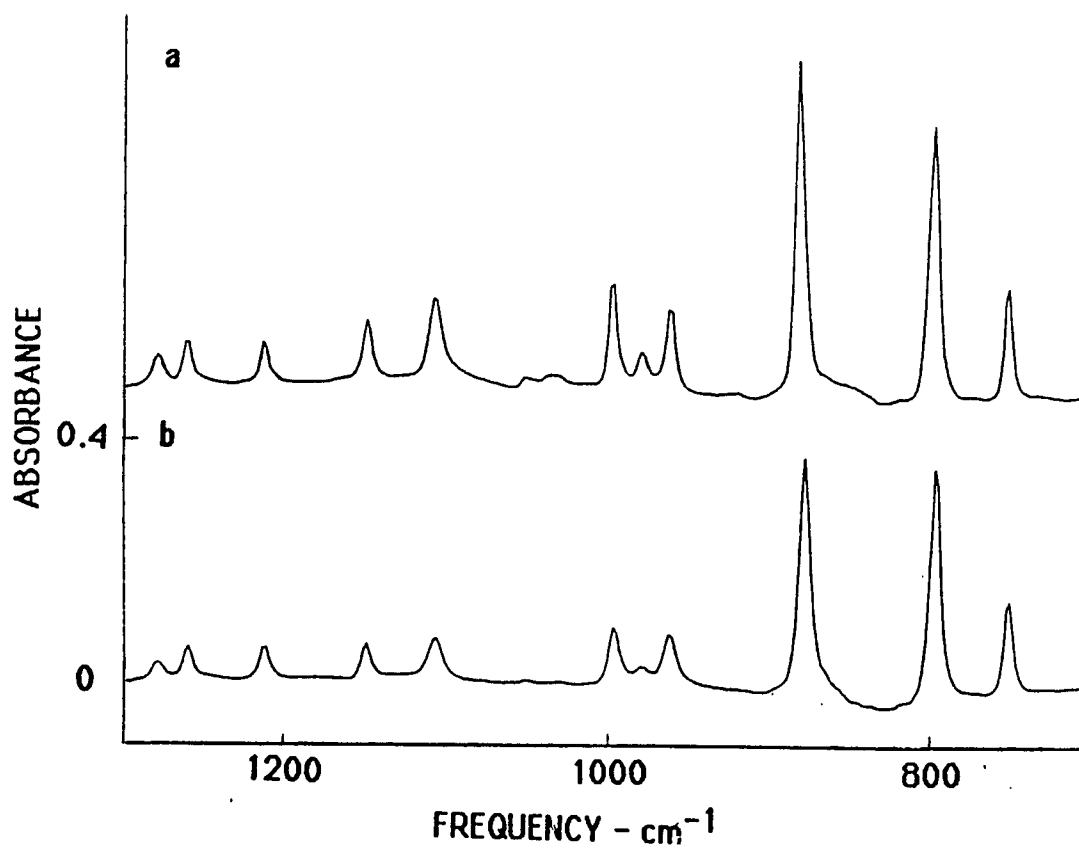
Subtraction of the amorphous component from each of the spectra obtained in the -145 to 60°C region was carried out using a spectrum taken for TPI at 65°C (Figure 5a), in order to obtain the spectra for 100% crystalline samples at low temperatures. The subtraction was successful for spectra taken at all temperatures except those below

-120°C. A comparison of the difference spectra for samples taken at -79 and at -145°C are shown for alpha and beta containing samples in Figure 20 a and b, respectively. Small broad bands are present in the latter spectra which could not be removed from the spectrum by subtraction.

Figure 20      SUBTRACTION OF AN AMORPHOUS COMPONENT  
FROM TPI SPECTRA AT LOW TEMPERATURES

Comparison of spectra obtained by subtraction of amorphous spectrum recorded at 65°c from spectra for trans-1,4 polyisoprene containing the beta crystalline form.

a. Spectrum taken at -78c. b. Spectrum taken at -120°c.



## DISCUSSION

### ASSIGNMENT OF TPI CRYSTALLINE SPECTRA

The infrared spectra for TPI are different for its two stable crystalline forms as well as for its amorphous state. The crystalline spectra contain sharp bands while the amorphous bands are broad. The spectrum for the alpha form contains more lines than that of the beta form. The conformational repeat unit for alpha TPI contains two chemical repeat units which pass through the crystallographic cell while beta has only one (5,6). The number of modes expected for each spectrum is related to the number of atoms per repeat conformational unit. The symmetry line group of a TPI chain is  $C_1$  in the two crystalline forms. This group contains no symmetry elements and therefore all the modes are expected to be infrared active.  $3N-4$  modes are observed for each crystal form, where  $N$  is the number of atoms per conformational repeat unit. Since alpha TPI has 26 atoms per repeat unit, 74

active modes are expected. For beta TPI, with 13 atoms, there are only 35 modes. The calculations for the vibrational frequencies show this number of modes.

For the alpha form many of the calculated modes in the CH stretching region at 3020- 2800  $\text{cm}^{-1}$  (Table III), appear twice with the same frequency or one slightly shifted. Each such pair of calculated modes with similar frequencies also has the same or similar potential energy distribution of normal coordinates. This indicates that they are probably due to the same vibrational mode in the two adjacent chemical repeat units. In the lower frequency region between 1700-900  $\text{cm}^{-1}$  most but not all the bands are paired. In this region each band contains contributions of mixed modes. The differences between a pair of calculated frequencies in this region are 1- 9 $\text{cm}^{-1}$  except for the pair calculated at 1559-1523  $\text{cm}^{-1}$ . The potential energy distribution for all these pairs of bands are also the same or similar. At the region below 900  $\text{cm}^{-1}$  each member of a pair is assigned to an observed frequency. The frequency difference between each pair of members in this spectrum

are  $9-52\text{ cm}^{-1}$  so that the splitting of the pair is large enough in this region so that both are observed. For the beta TPI spectrum the pairing does not occur and each calculated frequency corresponds to one observed value.

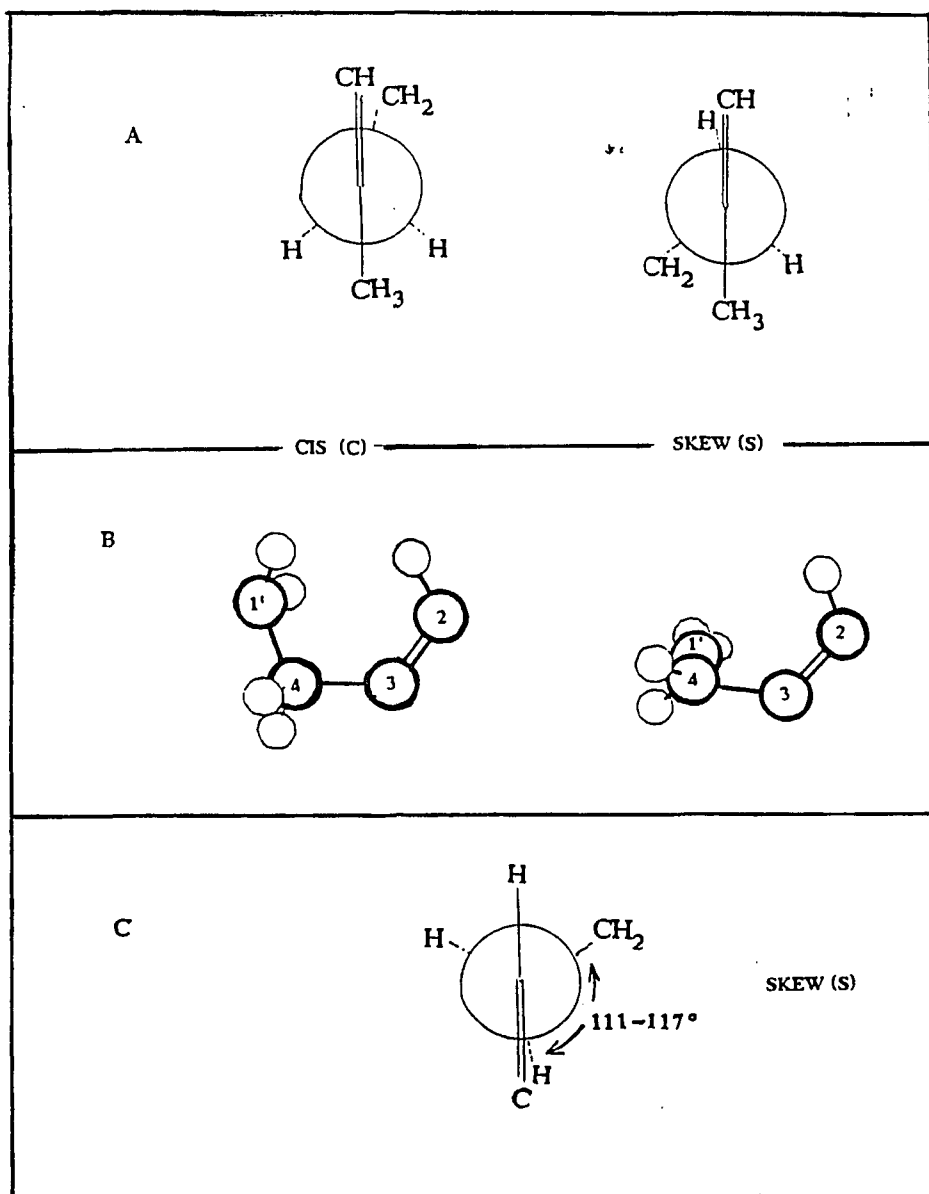
Another difference between the two forms is in the geometric parameters (bond lengths, bond angles and dihedral angles) which causes some difference in the orientation of the normal coordinates and as a result a shift in their corresponding vibrational frequencies (5,6). The differences in bond length for TPI in the two crystal forms are most apparent for the C=C bond. In the alpha form this bond is about 4% longer than in the beta. This geometrical difference is clearly reflected in the spectra, particularly in the C=C stretching band. Since this mode involves no other normal coordinates and there is no conformational difference between the two forms, the difference in their frequencies is due to this geometrical difference only. There is also a small difference between the single C-C bonds in the two forms but it can not be clearly shown in the spectrum since the stretching modes of

this group are mixed with other vibrations. No data are available for the exact positions of the hydrogen atoms in this structure and for this reason the same approximation was used to describe their geometry in the two forms. The bond angles differ for the two forms mainly in the  $C-C=C$  ( $\epsilon$ ) which is about 4% larger for the alpha form.

The main difference in geometry between the two TPI crystal forms is in the dihedral angle  $C_{(2)}H=C_{(3)}(CH_3)-C_{(4)}H_2-C_{(1')}H_2$ . This angle is approximately cis ( $8.6^\circ$ ) for the alpha form and skew ( $117^\circ$ ) for the beta. The difference between these two conformations leads to a large difference in interaction between the various normal coordinates in the structure. The Newman projection along the  $C_{(2)}(CH_3)-C_{(3)}H_2$  bond (Figure 21a), shows the effect of this rotational difference on the interaction between the methyl group and the methylene group whose carbon is three bonds away from it. This gamma-gauche effect ( $103^\circ$ ) is quite significant and should cause differences in the vibrational modes in the two geometries. Another effect of this bond rotation that can be seen in the same figure is that of the

Figure 21 CONFORMATIONS OF TPI REPEAT UNIT

Dihedral angle conformations in crystalline trans-1,4 polyisoprene.



interaction between the secondary carbon ( $C_1$ ) and the methylene group ( $CH_2(1')$ ). This rotation of the secondary carbon also leads to an interaction between the vinyl hydrogen and the same  $C(1'),H_2$  group which is different for the two crystal forms. This is shown in Figure 21b. Since the vinyl CH is four bonds away from the methylene group these groups are not expected to show any interaction effect; however, it can be seen that in the cis conformation these groups become very close to each other. Another interaction of the vinyl CH that should be considered is that CH with the  $C(4'),H_2$  group on the other side of the chain. This interaction is a result of the  $C(4'),H_2-C(1),H_2-C(2),H=C(3)$  dihedral angle rotation. This rotation is approximately gauche for both forms, however, the rotation is about 6 degrees smaller for the beta form. As a result, the fourth bond interaction is slightly weaker for the alpha form (Figure 21c). In addition this same rotational difference would also lead to a difference in the distance and the interaction between the methyl hydrogens and the methylene hydrogens on carbon 4a.

Although the carbons in the center of these two groups are in the same trans conformation around the rigid double bond in the two groups, the methylene rotation is different in the two cases since it involves a different dihedral angle.

Although differences in the number of chemical repeat units and in the geometries occur between alpha and beta TPI, the two forms are very similar. For this reason it should be possible to correlate these spectra and to account for the differences in the number of bands and their frequencies. Such a correlation is carried out in Table III by matching the calculated and observed frequencies for the two forms having the same or similar potential energy distribution. In most cases each frequency for the beta form is correlated to two alpha TPI observed bands and for a few bands the correlation is one to one. In only two cases does a substantial difference appear in the potential energy distribution for the correlated bands. These are for the calculated bands at 1361 (beta), 1346 (alpha) and at 174 (beta), 176 and 159  $\text{cm}^{-1}$  (alpha). It is observed that in most cases each frequency for the beta

form is associated with two calculated frequencies for the alpha form. There are four exceptions to this out of 35 calculated beta bands above  $170\text{ cm}^{-1}$ . There are two bands above  $170\text{ cm}^{-1}$  found for the alpha form only (observed at  $1579$  and  $1540\text{ cm}^{-1}$ ). In most cases the observed band intensities for the two forms are also approximately correlated, as seen in Figure 2. Exceptions occur where a band for beta TPI is associated with a single observed alpha TPI band at  $1050$ ,  $978$  and  $964\text{ cm}^{-1}$ . In all cases where the observed beta TPI band is associated with two observed alpha TPI bands, the combined intensities of the latter two approximate that for the former. It is concluded that there is a direct correlation between the two structures both in their vibrational frequencies and in their assigned potential energy distribution.

Many polymers have more than one stable crystalline form, containing one or more monomers per repeat conformational unit. Assuming that the correlation found for alpha and beta TPI has a general validity, it should be possible, using single-chain normal vibrational

calculations to correlate the spectra for the various forms of a particular polymer. For example, polyoxymethylene (104) is found in two crystalline forms. Form I with nine monomers and form II with four monomers per repeat conformational unit. Polyvinylcyclopropane (105,106) exists in form I containing nine monomers and form II containing four. Poly-1-butene I has 18 monomers and II has 44 monomers per repeat unit (107,108). Poly trimethylene oxide (109,110) has three stable crystal forms, I and III with four monomers and II with eighteen. Nylon 6 (111,112) has eight repeat units in the alpha form and four in the beta. Syndiotactic polypropylene (113,114) has four repeat units in crystal form I and two in II. For all these forms it is expected that each band in the spectrum of the crystal form with the smaller number of monomer units per repeat conformational unit should correlate to one or more bands in the spectra of the other forms containing more monomer units per conformational repeat unit. However, this correlation will not be so simple because in all the examples that were shown above, there is a symmetry to the

line group of the chain and it is different for each crystal form. For this reason many bands are optically inactive or the same group vibration appearing in the spectrum for each crystal form belongs to different irreducible representations; these effects may shift the two correlated frequencies away from each other and even switch their order with other bands. This can be shown very clearly for syndiotactic polypropylene (35). Crystal form I which contains four repeat units exhibits 26 optically active modes while form II with only two repeat units shows 50 modes. The reason for this is that in the first form the chain belongs to a higher line symmetry group ( $D_2$ ) compared to the latter ( $C_{2v}$ ). It is therefore not possible to correlate these spectra. TPI, on the other hand, shows a unique case in which the line group symmetry is  $C_1$ , which is the lowest possible for both forms. In this case all modes are active and their expected number is directly related to the number of atoms per repeat conformational unit. In addition, the low symmetry causes all modes to be in the same representation so that their vibrational bands

appear in the same order for the two TPI crystal forms.

#### ASSIGNMENT OF TPI AMORPHOUS SPECTRUM

It should be possible to extend the correlation between the infrared spectra for the two crystalline forms in TPI to a mixture of chain conformations as found in the amorphous state. Each single band in the beta TPI spectrum and the corresponding single or double bands in the alpha TPI spectrum should correlate with a series of amorphous bands belonging to the same vibration in different conformations which closely overlap or split into adjacent modes, appearing as a broad band.

The use of normal coordinate calculations for the assignment of the infrared spectrum of amorphous TPI is complicated by the large number of conformations that are present in this state. The C-C single bond conformations are restricted in the alpha and beta crystalline structure to single values for each bond, which results in the CTSCT $\bar{S}$  (cis, trans, skew, cis, trans, skew $\bar{}$ , starting with the =C-H carbon) conformational sequence for the alpha form and

the  $\overline{ST\overline{S}}$  sequence for the beta form. For amorphous TPI, on the other hand, other energetically allowed conformations are possible. The isomeric state approximation (115) can be used to calculate the most probable conformations for this form. This was done by assigning to each single C-C bond a small number of rotational states located at the minimum of their torsion potential. Calculations of the probability of the various sequences of these conformations can be used to divide them into three groups, reflecting their energies. The group with the most probable conformations includes extended TPI repeat units, with a trans configuration around their  $\text{CH}_2\text{-CH}_2$  bonds, while the other two bonds could be either cis or skew. The members of this group include  $\overline{STS}$ ,  $\overline{ST\overline{S}}$ ,  $\overline{CTS}$ ,  $\overline{ST\overline{S}}$ ,  $\overline{STS}$  and  $\overline{CT\overline{S}}$  conformational sequences. In the group of less probable conformations the TPI unit is folded since the  $\text{CH}_2\text{-CH}_2$  bond is in a gauche conformation while the two adjacent C-C single bonds have skew rotations (Figure 20a). The conformations in this group are  $\overline{S\overline{G}\overline{S}}$ ,  $\overline{S\overline{G}\overline{S}}$ ,  $\overline{S\overline{G}\overline{S}}$ ,  $\overline{S\overline{G}\overline{S}}$ ,  $\overline{S\overline{G}\overline{S}}$  and  $\overline{S\overline{G}\overline{S}}$ . Finally, the least probable group of conformations also includes folded TPI

repeat units with gauche conformation of the  $\text{CH}_2\text{-CH}_2$  bond, but with one of the bonds adjacent to it in the cis conformation while the other is skewed. This leads to a highly unstable geometry since the methyl becomes very closely spaced to the methylene group which is four bonds away from it (Figure 20b). This group includes CGS,  $\text{C}\bar{\text{G}}\text{S}$ ,  $\text{CG}\bar{\text{S}}$  and  $\text{C}\bar{\text{G}}\bar{\text{S}}$ .

The result of this difference in rotational structure is that for the crystalline modifications restriction of the position of each normal coordinate to one value leads to an infrared spectrum containing single sharp bands. When two positions exist for each coordinate, as described for the alpha TPI form, the infrared spectrum contains either singlets or doublets. The larger number of positions that is possible in the amorphous state, leads to an infrared spectrum containing groups of sharp singlets that overlap to form broad bands. However, since the possible single C-C bond conformations for the amorphous form include those that exist for the same single bonds in the alpha and the beta crystal structures, all of the spectral bands observed

for the crystalline TPI in the two forms should fall completely within the frequency domains of the amorphous bands. The intensity maximum of a particular crystalline band will not necessarily coincide with that for the amorphous band with the same assignment since chain units in other conformations undergoing the same vibrational mode could be more probable or the mode could have higher inherent intensity. Therefore the amorphous spectrum is assigned by a transfer of the potential energy distribution for the crystalline bands that are completely overlapped by an amorphous band. This correlation is shown in Table IV , along with band assignments for the amorphous bands. For the  $1450\text{ cm}^{-1}$  bands two separate overlapping modes are assigned. As noted above, alpha and beta have different assignments for the  $1348, 1340\text{ cm}^{-1}$  bands ( $1329\text{ cm}^{-1}$  for the amorphous). The  $1051$  (alpha and beta),  $1033$  (amorphous) and the  $962$  (beta),  $964$  (alpha),  $924$  (amorphous) are mixed modes. Some of the amorphous bands such as those at  $3015, 2975, 1665, 1450, 1430, 1383, 1281, 1253$  and  $1150\text{ cm}^{-1}$  have their maxima at the same or similar frequencies as those

for both corresponding crystalline bands. In other cases, although overlap occurs the correlation is not apparent, since the maxima in the crystalline spectra are shifted considerably from those in the amorphous spectrum. Examples are shown in Figure 7 and include the amorphous band at 842  $\text{cm}^{-1}$  with shoulders at 860 and 884  $\text{cm}^{-1}$ , assigned to the vinyl C-H out of plane bending, and the doublet at 1220, 1206  $\text{cm}^{-1}$ , assigned to the C-H in plane bending. The amorphous bands, as assigned, are observed to overlap the alpha and the beta bands having the same assignments. In three cases amorphous bands correspond to two observed alpha TPI bands (the amorphous bands at 1253, 1099 and 800  $\text{cm}^{-1}$ ). The intensities of corresponding amorphous and crystalline bands approximately agree as shown in Table IV.

After the assignment of the amorphous bands was complete, it was of interest to study the components, or the sharp amorphous bands that compose the band envelopes in the amorphous spectra. This was done by following the changes that occur in the band contours as the temperature is raised above  $T_m$ . The spectral band changes indicate that

conformational changes occur at these temperatures, with different conformations becoming preferred. The bands that show this change in contour include the vinyl C-H out of plane bending mode with at least three components at 842, 860 and 884  $\text{cm}^{-1}$  and the C-H in plane bending modes with at least two components at 1205 and 1220  $\text{cm}^{-1}$ . The asymmetric band at 1099  $\text{cm}^{-1}$  and the shoulder at 800  $\text{cm}^{-1}$  also appear from these studies to be conformationally sensitive. Furthermore, the two bands at 976 and 987  $\text{cm}^{-1}$ , previously assigned to two different modes (Table III), are now believed to be components of the same  $\text{CH}_3$  rocking mode. In making the conformational assignments of these components it is assumed that the conformational changes that require less energy will be more prevalent at lower temperatures. In particular, the change in the  $\text{CH}_2$ - $\text{CH}_2$  bond rotation angle from a trans to a gauche conformation is expected to be observed first and to have the most significant effect on the band contours. This will change the extended amorphous repeat units into folded ones. At the same time the band components associated with the gauche conformation

at the  $\text{CH}_2\text{-CH}_2$  bond will show changes at higher temperatures. In this way, the components which change right above  $T_m$  were assigned to the trans conformation which belongs to the most probable group of conformations. Components which gradually continue to change also at higher temperatures were assigned to gauche conformations. Finally, those components that do not change at all through the temperature range of the experiment were associated with the least probable group also with a gauche conformation. It is also expected that those parts of the amorphous bands which are associated with the  $\text{CH}_2\text{-CH}_2$  sequences that are in the trans conformation will have frequencies close to those for the crystalline forms which are also extended. The assignment can be clearly seen for the 1204-1220 and for the 976-987  $\text{cm}^{-1}$  band components. The greater intensity change that occurs right above  $T_m$  at the 1204  $\text{cm}^{-1}$  component in the first case is used to assign it to the trans conformation. The 1220  $\text{cm}^{-1}$  component of this band changes gradually at higher temperatures and it is therefore assigned to the less probable group of folded

conformations. In the same way, the 976  $\text{cm}^{-1}$  component is assigned to the trans and the 987  $\text{cm}^{-1}$  to the gauche conformation in the latter band. The assignment of the amorphous band with a maximum at 842  $\text{cm}^{-1}$  was more complicated. The components at 882 and 860 show a large change in intensity with temperature right above  $T_m$  and a smaller change at higher temperatures and are therefore assigned to the trans conformation. Two other components at 868 and 890 are also assigned to the trans conformation although they do not show a large intensity change right above  $T_m$ . This assignment is made because these bands are in the frequency region in which the bands for the two crystal forms occur. The 844 and 838  $\text{cm}^{-1}$  components of this band show a gradual change at higher temperatures and are therefore assigned to the folded gauche conformation. The 824  $\text{cm}^{-1}$  component of this band shows no change at all throughout the temperature range of this experiment and is therefore assigned to the least probable group of conformations containing the cis-gauche-skew sequence. Deconvolution of the components of these three amorphous

bands at 840-890, 970-990 and 1205-1235  $\text{cm}^{-1}$  yielded frequencies in agreement with those given in Table V. The intensity shifts occurring in the 1664-1672  $\text{cm}^{-1}$  band, assigned principally to C=C stretching, are not believed to be due to conformational changes. There is a bond length difference of about 4% between the alpha and the beta forms, which causes a shift in the vibrational frequency. The average C=C bond length in amorphous TPI is not known but the current result suggests that it differs slightly from either of the two crystalline forms.

Conformational assignments were given previously for polyethylene and polybutadiene. For polyethylene Snyder (30) established the values of absorbance frequencies of various chain conformation sequences. This was done using low molecular weight paraffins in the liquid state. However this work did not assign either the high molecular weight paraffins or polyethylene in the amorphous state. The reason for this, as stated by the authors is that the band components due to the many conformations in the amorphous state could not be separated. Later workers did attempt to

separate these band components. Ungar and Organ (116) used Snyder's assignments to assign band components. Their technique is similar to the present work for TPI. The intensity changes of the different band components are followed as the sample temperature is changed. However, the band components were separated by deconvolution which involves assumptions about line shapes and mathematical approximations and the assignments were not made by subtraction of spectra. In the work on polybutadiene (64), the changes in different band component intensities were used to establish their conformational assignment by determining whether the repeat units are extended or folded. However, the technique used to separate the different components was again deconvolution. In addition, only one spectral band was used without following the changes that occur in the rest of the spectrum. In the present work, deconvolution was used only to confirm the results. The changes in the band components are observed in the spectrum itself (Figure 8) and the subtraction is used only to clarify these changes (Figure 9).

## SURFACE REACTIONS

Epoxidation and hydrochlorination of TPI lamellas in suspension have been previously used to determine the average number of monomer units per fold in these structures (7,8,90). In order for this method to be successful, reaction of all the surface component but no penetration of the crystal core must occur. The absence of amorphous TPI components after reaction would show that all of this component was initially present at the surface and that all of it has reacted. Infrared spectra are used in this work to show that indeed the reaction was complete at the lamellar surfaces since no unreacted amorphous TPI bands are observed.

Other methods have been shown to be useful in monitoring surface reactions. The two methods used previously for TPI were heat of fusion measurements from differential scanning calorimetry (90) and solid state NMR experiments (117). For epoxidized TPI samples which were prepared under the same conditions as those used in the

present work, the heat of fusion remained constant for TPI lamellas with reacted and unreacted surfaces (90).

Measurements on samples reacted under different conditions (by using a different reaction liquid) resulted in a decrease in the heat of fusion with increasing fraction of epoxidation above a fraction corresponding to complete surface reaction. Another method that was found useful to monitor surface reactions was solid state NMR. Preliminary work (117) was carried out for TPI. In the NMR method the amorphous component observed for each carbon atom diminishes and a new resonance due to surface epoxidation is observed. However the use of FTIR for this purpose is experimentally simpler and each newly reacted surface component exhibits a new spectrum that can be separated by subtraction from that for the crystal core.

The application of pressure to a surface reacted TPI lamellar sample, previously shown to cause a decrease in sample crystallinity in unreacted samples (118), results in the appearance of amorphous bands which were subtractable. Since before the application of pressure, only a

crystalline and a chemically modified surface component were present, the appearance of bands characteristic of amorphous TPI shows in a direct way conformational changes in portions of the crystalline core.

The surface modification of TPI lamellas is reflected in three types of changes in its infrared spectrum. i) The disappearance of all modes which directly involve the C=C group vibrations. ii) The appearance of new modes that are due to the vibrations involving the chemical groups that were added to the double bond, the epoxy group, C-C, in one case and the C-Cl group in the other. iii) Changes that occur in the rest of the modes of groups that were not chemically altered by this reaction. For amorphous TPI the bands involving the C=C group that should disappear are those at  $1665\text{ cm}^{-1}$  (C=C stretching),  $1220$  and  $1205\text{ cm}^{-1}$  (=C-H in plane bending),  $884$ ,  $862$  and  $842\text{ cm}^{-1}$  (=C-H out of plane bending),  $595$  and  $570\text{ cm}^{-1}$  (C=C-C bending) and  $520$ - $<505\text{ cm}^{-1}$  (=C-CH<sub>3</sub> out of plane bending). The epoxidation and the hydrochlorination reaction conditions used in the present work clearly cause the loss of these bands from the

amorphous spectrum. In some cases, however, an amorphous band is replaced by one or more new bands in the same general frequency region. For example, the bands at 595 and 570  $\text{cm}^{-1}$  are replaced by one at 565  $\text{cm}^{-1}$  in surface hydrochlorinated material and at 540  $\text{cm}^{-1}$  in surface epoxidized TPI. New bands appear in the spectra for surface reacted TPI as expected. Bands at 1250, 1122 - 1069 and 700 - 685  $\text{cm}^{-1}$  are tentatively assigned (112) to symmetric epoxy ring stretching, asymmetric epoxy stretching and epoxy ring deformation, respectively. Bands at 635 and 565  $\text{cm}^{-1}$  are both attributed to C-Cl stretching (35-39).

Other vibrational modes in the modified spectra were only slightly different and correlate closely with those of amorphous TPI. Bands of this type are mainly due to  $\text{CH}_2$ ,  $\text{CH}_3$  and C-C vibrations and their combinations. For the epoxidized TPI spectrum, these correlated bands include also out of plane bending modes since the rigid double bond conformation is retained in the structure after the reaction by the oxirane ring. These include the 880  $\text{cm}^{-1}$  band that is assigned to out of plane bending of the

hydrogen on the epoxy ring and is correlated to the 840  $\text{cm}^{-1}$  band that is due to the same type of vibration of vinyl hydrogen in TPI. The same correlation applies to the 540  $\text{cm}^{-1}$  epoxy band and the 520 - <505  $\text{cm}^{-1}$  doublet that are assigned to the out of plane bending mode of the methyl group. For the hydrochlorinated TPI spectrum there are some differences in relative intensities for the methylene bands. The larger intensity is observed for the hydrochlorinated bands and they are apparently due to the additional methylene group that is present in this modified product as a result of the addition to the double bond. The intensity change is most apparent in the TPI bands at 1307  $\text{cm}^{-1}$  (1305  $\text{cm}^{-1}$  hydrochlorinated), 1253  $\text{cm}^{-1}$  (1261  $\text{cm}^{-1}$  hydrochlorinated) and 1150  $\text{cm}^{-1}$  (1150, 1140  $\text{cm}^{-1}$  hydrochlorinated) which were assigned previously to methylene wagging and twisting modes and in the 764 - 746  $\text{cm}^{-1}$  TPI bands (746  $\text{cm}^{-1}$  hydrochlorinated) band due to the methylene rocking. The weak bands at 1234, 876, 855, 837 and 684  $\text{cm}^{-1}$  for surface epoxidized TPI are unassigned.

The method of assignment by surface modification is

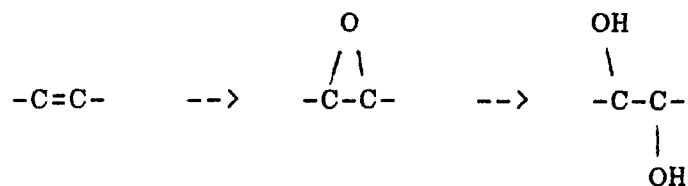
similar to that of deuterium substitution in that they both use chemical modifications for assignment verification. Deuterium substitution is used to verify assignments for polymer spectra (30,33,47) by following the shifts in the spectral bands. Deuteration is very useful since when it is done selectively it results in simple spectral changes. The advantage of the use of surface modification is that each reaction could be used for assignments of modes due to several groups at the same time. For example, the epoxidation of the double bond in TPI can be used to verify assignments for the double bond vibrations as well as for the vinyl hydrogen and methyl and for the C=C-C bending modes. In addition, different reactions can be used to verify the same assignments independently. In the present work, the use of surface reactions was advantageous since they were previously carried out and the identity of their product was established by NMR studies (7,8).

Attempts were made to carry out a new surface modification reaction on TPI lamellas. The reaction was the conversion of the TPI double bond into a diol. The

hydroxylation product has not yet been characterized unequivocally and only infrared spectral results are presented in this work. The infrared spectrum (figure 13b) of the reacted surface supports the fact that it is probably a TPI diol. The spectrum contains a large and broad band at  $3040\text{ cm}^{-1}$  assigned to OH stretching. The band due to in-plane bending of the hydroxyl hydrogen is believed to occur at  $1372\text{ cm}^{-1}$ . Two intense overlapping bands at  $1072$  and  $1028\text{ cm}^{-1}$  are attributed to the C-O stretching mode at the tertiary and the secondary carbons respectively (119). Other bands in the hydroxylated spectrum are only slightly different and correlate closely with those in amorphous TPI. These bands, listed in table VII, are mainly due to  $\text{CH}_2$ ,  $\text{CH}_3$  and C-C vibration and their combinations.

The conversion of the double bond into a diol can take place by two different routes. These are the anti addition, in which each hydroxyl group adds to the double bond from a different side (98, 120-123), and the syn addition, where the two groups add from a the same side of

the double bond(98,124-129) . The anti 1,2-diol is believed to form in two steps, via an epoxide intermediate:



The advantage of using this reaction is that the epoxidation reaction of TPI was studied extensively in the past(2,90). One problem with the diol formation by anti addition is that the hydroxylation step takes place by a reagent attack from both sides of the double bond, and may not occur in a reasonable amount of time due to the hindered structure of the chain folds. The hydroxylation step which includes the opening of the oxirane ring can take place either by acid or by base catalysis. While the basic route is extremely slow (130), the acidic reaction is susceptible to side reactions. One of the most common side reactions is Pinacol rearrangement (98) in which the diol rearranges into a ketone. This type of reaction is especially common for tertiary carbons. Another possible side reaction is the addition of a nucleophile from the

acid to one of the carbons in place of an hydroxy group (98). In the case when the ring opening is carried out in solution, cyclization can take place (131,132). This can occur by the reaction of the double bond at the unreacted TPI segments.

In order to eliminate these problems, syn addition was chosen for this work (133). The reaction was carried out in two steps. The first step is the addition of osmium tetroxide to the double bonds available for reaction at the lamellar surfaces and the second step includes transesterification of the osmate leading to diol formation using mannitol. The two reaction steps take place from the same side of the double bond.

The result of the fact that the second step involved a dissolution of the polymer is seen in its FTIR spectrum. The product did not contain only unreacted crystalline TPI and modified amorphous TPI components. The spectrum showed both crystalline and amorphous TPI components as well as hydroxylated TPI bands.

The hydroxylated product has not been completely

identified to date since its NMR spectrum was not obtained. The reason for this is the low solubility of this product in most solvents.

#### CRYSTALLINITY MEASUREMENTS FROM IR SPECTRA

The results of the crystallinity measurements using the infrared method developed in this work were compared with those from density measurements for seven preparations of unfractionated TPI with different morphologies and crystal structures. These measurements were shown to be in agreement within two percent. Infrared crystallinities were obtained (90) for fractionated samples; a comparison with density measurements and with the fraction reacted by the surface epoxidation/ C13 NMR method showed an agreement within 0.03 units for the three methods.

Infrared measurements were also used to quantitatively measure the decrease in crystallinity that occurs in TPI lamellar samples upon application of a minimum measureable pressure of 200 psi. These results are in quantitative agreement with density measurements that

preceded this work and that show a decrease in crystallinity of about 5-7% for TPI lamellar mats (118).

The successful use of infrared spectroscopy, as developed in this work, to determine sample crystallinity is believed to be a consequence of the choice of the C=C stretching band with maxima at 1664-1672  $\text{cm}^{-1}$  for the different samples. This band is separated from other bands and therefore its area can be measured directly without deconvolution. In this way any assumptions and approximations resulting from peak separation are eliminated. This band also has a clear baseline which can be determined unambiguously. For this particular normal mode, it is found that the band envelopes of the alpha and beta crystalline and the amorphous spectra are almost constant in position and in band width. For this reason, in semicrystalline TPI a single band is observed. The area for this infrared band is independent of crystallinity from at least 50 to 0%, and this area depends only on the amount of material present and therefore on the sample thickness. The constant position of the band envelope and its

independence of crystallinity changes at constant sample thickness, is believed to be due mainly to the constant geometry of the C=C bond, which is held in the trans configuration. Out of all the carbon-carbon bonds that are included in TPI chain backbone, only the C=C bond has the same local conformation in both the two crystalline arrangements and in the amorphous state. A small shift in the vibrational frequency of this band in the two crystalline forms does occur because of the difference in the C=C bond length in the two crystal forms.

The advantage of this infrared method is that it is experimentally simple, independent and does not involve any approximations. Most crystallinity measurements using infrared spectroscopy (11,81,82) are more complicated. These methods are not direct since they involve measurements of some samples whose density must be known. In addition, the crystallinity is determined by extrapolation to a particular value which involves approximations. The method that is presented in this work is extremely useful for diene polymers. However, in order

to apply it to other polymers it would be necessary to find vibrational bands whose absorbance coefficient is the same in the crystalline and in the amorphous states.

Another method for measuring crystallinity is the determination of the amorphous content in the spectrum using the subtraction factor necessary to remove all the amorphous bands of a given sample and to obtain a 100% crystalline sample. This method was used to obtain measurements of sample crystallinity at different temperatures. The subtraction factor for a particular sample is ratioed against the factor found for a spectrum of the same sample at room temperature. The crystallinity of the latter is known by measuring the crystalline fractional area of the C=C stretching band as described above. The results of these measurements indicate that for both alpha and beta TPI samples the amorphous content decreases by about 10% as the temperature is lowered from 25 to about  $-30^{\circ}\text{C}$ . The samples that were used for this experiment were stacks of curved lamellas in the beta form with 8-11 monomer units per fold (90). Since beta TPI

single lamellas contain folds with average length of 8-9 monomer units (90) the amorphous chain units in curved lamellar structures, are principally in the chain folds. These values were obtained from surface epoxidation experiments at 0°C. The surface fractions from the C-13 NMR measurements were the same as those from density and FTIR measurements at room temperature. However, no correction in the C-13 NMR values was made for the fact that the fraction epoxidized is expected to be too high due to epoxidation of all the double bonds on the lateral crystal edges as well as those in the folds. Since the average length of the crystalline stem is about 16 monomer units (90), a 10% decrease in the amorphous content is interpreted as a change in conformation of an average of two monomer units per fold into a crystalline conformation identical to that found in the lamellar core. At the same time the average fold length becomes shorter by two units. It is assumed that the conversion into the crystalline conformation occurs at the amorphous units which are nearest the crystal stems since the crystalline monomeric units already present

are in a low energy state. In modelling the conformations at the crystalline folds the amorphous segments near the crystal stems are expected to be in extended conformations (CTS or STS) which are different from that in the crystal core (134). Along with this a change probably occurs in the conformations of units that were previously folded to extended amorphous conformations keeping in this way the overall average amorphous conformation approximately constant. The retention of the overall conformation of the folds is reflected in the constant infrared band contour observed at all temperatures.

The possibility that these spectral changes were artifacts of the spectrometer optics and did not reflect real changes in the sample was carefully considered . However, the increase in crystallinity is not continuous as the temperature is lowered. Under  $-30^{\circ}\text{C}$  the amount of amorphous content for a given sample levels off and becomes constant. This fact is true for both alpha and beta samples. Another indication is in the fact that the crystallinity changes in the samples are reversible and as

the samples are warmed above  $-30^{\circ}\text{C}$  their amorphous content increases gradually at about the same amount per degree as that in which it had decreased in the cooling experiment. Finally, these results are shown to be continuous also in a separate experiment done above room temperature, and an increase is observed in the amorphous content as the sample is heated to  $60^{\circ}\text{C}$ , a temperature close to but below the melting point. Up to about  $40^{\circ}\text{C}$  the amorphous content changes at the same amount per degree as that observed below room temperature. Above  $40^{\circ}\text{C}$  more crystalline units are observed to change their conformation per degree. This type of change, referred to as premelting, has been observed for melt-crystallized polyethylene (135,136). The increase in amorphous content for polyethylene was found by low angle X-ray scattering to be accompanied by first a decrease in the average crystal stem length and then, close to the melting point, an increase in this parameter while the thickness of the amorphous and the "transition" layer increased over the whole temperature range.

The results of the present work clearly indicate that

the crystallinity for TPI lamellas is a function of temperature between  $-30^{\circ}\text{C}$  and the melting point. It is also believed that in the temperature region of  $-30$  to  $+25^{\circ}\text{C}$  these changes are occurring near the interface between the crystalline stem and the surface fold where the amorphous units are found in an extended conformation, and where the interconversion from crystalline to amorphous conformations should require small amounts of energy.

The results above room temperature do not preclude crystals melting from the side, particularly in the  $40-60^{\circ}\text{C}$  region which is close to the melting point. At this temperature range the conversion is not expected to be only slow and gradual at the crystalline amorphous interface.

The decrease in amorphous content which is interpreted in this work as the tightening of the traverse folds in TPI lamellas supports a lamellar model containing adjacent loose folding with little nonadjacent reentry of chain folds (137,138,139). At low temperature the adjacent chains take on a crystalline conformation and in this way the crystal component grows while the fold becomes tighter.

From the results to date it does not appear that all of the folds are tight and adjacent; this state would correspond to a fold length of 3-4. Some nonadjacent reentry to nearby stems is still possible. For a similar polymer, trans-1,4-polybutadiene containing 1% cis the fold length varies from 5 to 9 units depending on crystallization temperature. The melting point of this polymer is about 70 degrees higher than for TPI and therefore changes in crystallinity below room temperature are not expected. The change in fold length with temperature for trans-1,4-polybutadiene is attributed to rejection of cis units and nearby trans units from the crystal core (140).

#### TPI IR SPECTRA AT LOW TEMPERATURES

As the temperature is lowered from room temperature there are some changes in the semi-crystalline spectra of TPI. These are more significant for the beta than for the alpha TPI spectrum. All bands increase in intensity with decreased temperature while in some of them narrowing also occurs. This phenomenon had been reported for other

polymers (75-79) and explanations for it given in term of the change in the intermolecular spacing that causes an increase in the dipole- dipole interaction. Another reason for the increase in intensity, according to the past work, is the change in the lattice potential as the molecules get closer together which increases the vibrational force constants. These changes also cause small shifts in some of the bands (80).

For TPI the change in the intermolecular spacing at low temperatures brings about a splitting of the  $1450\text{ cm}^{-1}$  band. This band was assigned by calculations (Tables III and IV) to two separate pure vibrational modes which overlap. One is the assymmetric methyl bending which involves only one normal coordinate that contributes over 90% of the potential energy distribution of some of the overlapping bands in this frequency. The other overlapping mode is the methylene scissoring for which calculations show over 60% contribution of  $\text{CH}_2$  bending to the potential energy distribution and about 20% total of two CCH bending modes. The splitting of the overlapping bands into these

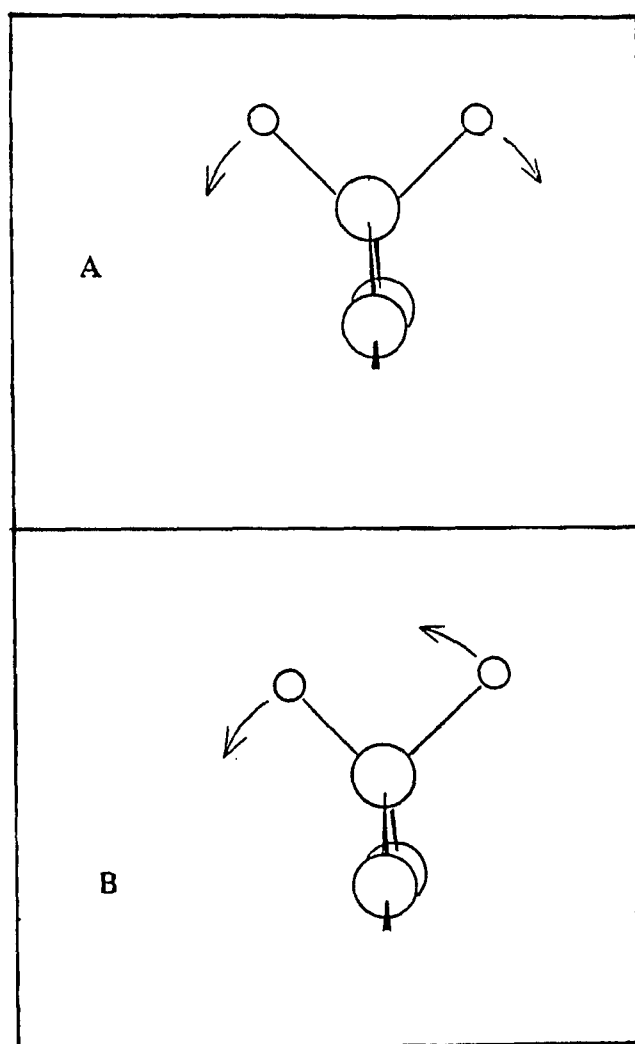
two modes starts to occur a few degrees below room temperature. First, a shoulder appears and then, at lower temperature two separate bands of unequal intensity are observed. The higher frequency band is assigned to asymmetric methyl bending and the lower one to methylene scissoring. At temperatures below  $-120^{\circ}\text{C}$  another splitting occurs into two components of equal intensity which is attributed to the methylene scissoring. This type of splitting had been reported for many polymers (141,142,143) and it occurs either at room temperature or lower. It is a result of the decrease in interchain distance. At low temperatures the chains become close enough so that the symmetry of the whole cell becomes effective in determining the optical activity of its vibrational modes. In the case of beta TPI the single chain is in the  $C_1$  line group. The space group for the TPI chain in the orthorombic crystallographic cell is  $D_2$ . For polyethylene (140,141) and polybutadiene (142) the spacing between adjacent chains is smaller and therefore this effect is apparent at ambient temperature. For polyisoprene it can be seen only at a much

lower temperature. The interchain effect is always observed first for methylene modes in polymers, in particular for the scissoring and the rocking vibrations. The reason for this is in the nature of the vibration (Figure 22) in which the hydrogen atoms move away from the chain. Scissoring and rocking are modes of the same type which differ only in the relative direction of the hydrogen motion. Wagging and twisting do not cause the methylene hydrogen to move away from the chain. In addition, the scissoring appears usually at higher temperatures than the rocking mode. For example, for polybutadiene (45) at room temperature only the methylene scissoring band splitting is observed while at lower temperatures also the rocking band splitting can be seen. For TPI only the methylene scissoring band is observed to be split while it is expected that at lower temperatures also the rocking mode will show splitting. The reason for this is probably in the geometry of these modes (Figure 22). This is probably a result of the fact that for the scissoring vibration the two methylenes move away from each other while in the rocking mode they move in the same

Figure 22 METHYLENE BENDING

Methylene bending modes in a polymer chain. A) Scissoring.

B) Rocking.



direction. Splitting modes for methyl bending and rocking are never observed; in these vibrational modes the hydrogens move inward towards the center of the group and not outwards which would place them closer to the other chains.

### CONCLUSIONS

The following conclusions can be drawn from this investigation:

- (1) FTIR spectra for 100% crystalline alpha and beta TPI can be obtained and assigned.
- (2) There is a correlation in the observed frequencies and the calculated potential energy distribution of alpha and beta TPI spectra.
- (3) The spectrum of amorphous TPI can be assigned by the transfer from band assignments of correlated crystalline bands.
- (4) Assignments can be made for the components of some conformationally sensitive amorphous bands.
- (5) Infrared spectra for some modified TPI lamellar surface can be assigned.
- (6) Hydroxylation of the double bond on TPI lamellar surfaces can be partially carried out.
- (7) The percent crystallinity of semicrystalline TPI samples can be measured from the infrared spectra.

- (8) The crystallinity of TPI increases with decreased temperature in the range between  $-30$  and  $+60^{\circ}\text{C}$ .
- (9) The interchain distance in crystalline TPI decreases at low temperatures and this change can be followed by infrared spectroscopy.

REFERENCES

1. A. Keller and E. Martuscelli Makromol. Chem. 151, 189 (1972).
2. K. Anandakumaran, W. Herman and A. E. Woodward, Macromolecules 16, 563 (1983).
3. C. Kuo and A. E. Woodward, Macromolecules 17, 1034 (1984).
4. J. Xu and A. E. Woodward, Macromolecules 19, 1114 (1986).
5. Y. Takahashi, T. Sato, H. Tadokoro and Y. Tanaka, J. Polym. Sci., Polym. Phys. Ed. 11, 233 (1973).
6. C. W. Bunn, Proc. R. Soc. London, Ser.A 8, 497 (1942).
7. F. C. Schilling, F. A. Bovey, K. Anandakumaran and A. E. Woodward, Macromolecules 18, 2688 (1985).
8. F. Tischler and A. E. Woodward, Macromolecules, 19, 1328 (1986).
9. A. E. Woodward, Preparation of Block Copolymers by Chemical Reactions on Lamellas of Partially Crystalline Flexible Polymers, from: C. E. Carraher and J. A. Moore Modification of Polymers (Plenum, New York, 1983).
10. S. Tseng, W. Herman, A. E. Woodward and B. Newman, Macromolecules, 15, 3338 (1982).
11. B. Wunderlich, Macromolecular Physics, Vol. 1 (Academic Press, New York, 1972).
12. W. Cooper and G. Vaughan, Polymer, 4, 329 (1963).

13. D. Fisher, Proc. Phys. Soc.(London), B66, 7 (1953).
14. Springer Advances in Polymer Science, ( Vol 54, 1985), J. L. Koenig Fourier Transform Infrared Spectroscopy of Polymers.
15. H. W. Siesler, J. Mol. Structure, 69, 15 (1986).
16. R. A. Saunders and D. C. Smith, J. Appl. Phys. 20, 953 (1949).
17. G. B. B. Sutherland and A. V. Jones, London Farad. Soc. 9, 281 (1950).
18. M. A. Golub, J. Polymer Sci. 36, 523 (1959).
19. I. Kossler and J. Vodehnal, J. Polymer Sci.B 1, 415 (1963).
20. J. L. Binder, J. Polymer Sci, A 1, 47 (1963).
21. V. N. Nikitin and B. Z. Volcheck, Zh. Prikl. Spektroskopii Akad. Nauk Bellorussk. SSR, 4, 546 (1966).
22. M. A. Golub, Spec. Acta, 26A, 1883 (1970).
23. S. W. Cornell and S. W. Koenig, Macromolecules, 2, 546 (1969).
24. R. J. Pectavich and M. M. Coleman, J. Polym. Sci., Polym. Phys. Ed. 16, 2097 (1980).
25. J. L. Koenig, Appl. Spec., 29, 293 (1975).
26. Methods in Experimental Physics, 16A, chap. 3., R. G. Snyder, Infrared and Raman Spectra of Polymers (Academic Press, New York, 1980).

27. M. M. Coleman and P. C. Painter, *J. Macromol. Chem.*, C16, (2), 197 (1978).
28. M. M. Coleman, P. C. Painter, D. L. Tabb and J. L. Koenig, *Polym. Lett.*, 12, 577 (1974).
29. P. C. Painter and J. L. Koenig, *J. Polym. Sci. Polym. Phys. Ed.* 15, 1885 (1977).
30. R. G. Snyder, *J. Chem. Phys.* 47, 1316 (1967).
31. C. G. Opaskar and S. Krimm, *Spectrochim. Acta* 21, 1165 (1965).
32. M. Gussoni, S. Abbate and G. Zerbi, *J. Chem Phys.* 71(8), 3428, (1979).
33. R. G. Snyder and J. H. Schachtschneider, *Spectrochim. Acta*, 20, 853 (1964).
34. J. H. Schachtschneider and R. G. Snyder, *Spectrochim. Acta*, 21, 1527 (1965).
35. T. Miyazawa, Y. Ideguchi and K. Fukushima, *J. Chem. Phys.*, 38, 2709 (1963).
36. S. Krimm, *Pure Appl. Chem.* 16, 369, (1968).
37. A. Rubcic and G. Zerbi, *Macromolecules* 6, 751, (1974).
38. A. Rubcic and G. Zerbi, *Macromolecules* 6, 759, (1974).
39. D. L. Tabb and J. L. Koenig, *J. Pol. Sci. Polym. Phys. Ed.* 13, 1159 (1975).
40. M. Kobayashi, K. Tashiro and H. Tadokoro, *Macromolecules*, 8, 158 (1975).
41. T. Shimanouci and B. Tasumi, *Bull. Chem. Soc. Japan* 34, 359 (1961).

42. M. Tasumi and T. shimanouchi, *Polymer J.*, 2, 62 (1971).
43. C. Y. Liang and S. Krimm, *J. Chem Phys.* 25, 563, (1965).
44. N. Neto and C. DiLauro, *Eur. Polym. J.* 3, 645, (1967).
45. S. L. Hsu, W. H. Moore and S. Krimm, *J. Appl. Phys.* 46, 4185 (1975).
46. M. M. Coleman, D. L. Tabb, B. L. Farmer and J. L. Koenig, *J. Polym. Sci. Polym. Phys. Ed.* 12, 445 (1974).
47. K. Holland-Moritz and K. Van Werden, *J. Polym. Sci. Polym. Phys. Ed.* 18, 1753 (1980).
48. P. C. Painter and J. L. Koenig, *J. Polym. Sci. Polym. Phys. Ed.* 15, 1885 (1977).
49. P. C. Painter and R. G. Snyder, *Polymer* (1981).
50. K. Fukushima, Y. Ideguci and T. Miyazawa, *Bull. Chem. Soc. Japan*, 36, 1301 (1963).
51. V. D. Gupta, S. Tevino and H. Boutin, *J. Chem. Phys.* 48, 3008 (1968).
52. Y. Abbe and S. Krimm, *Biopolymers*, 11, 1817 (1972).
53. S. Krimm, Peptides and Proteins, in T. G. Spiro, Biological Applications of Raman Spectroscopy (John Weiley and Sons, New York, 1987).
54. W. H. Moore and S. Krimm, *Makromol. Chem. Suppl.* 1, 491 (1975).
55. V. G. Boitsov and Y. Y. Gotlib, *Opt. Spectrosc. USSR. Suppl.* 2, 65 (1966).

56. S. W. Cornell and J. L. Koenig, *Macromolecules* 2, 540 (1969).
57. M. M. Coleman, P. C. Painter and J. L. Koenig, *J. Raman Spect.* 5, 417 (1976).
58. W. H. Moore and S. Krimm, *Makromol. Chem. Suppl.* 1, 491 (1975).
59. G. Zerbi and M. Sacchi, *Macromolecules*, 6, 692 (1973).
60. G. Masetti, F. Cabassi, G. Morelli and G. Zerbi, *Macromolecules*, 6, 700 (1973).
61. G. Zerbi, *Pure Appl. Chem.* 236, 499 (1971).
62. G. Zerbi, L. Pisseri and F. Cabassi, *Mol. Phys.*, 22, 241 (1971).
63. T. Shimanouchi, Y. Abbe and M. Mikami, *Spectrochim. Acta*, 24A, 1037 (1968).
64. T. Oyama, K. Shiokawa and Y. Murata, 6, 549 (1974).
65. S. J. Spell, S. J. Organ, A. Keller and G. Zerbi, *Polymer*, 28, 697 (1987).
66. X. Jing and S. Krimm, *Polymer*, 20, 1155 (1982).
67. J. Mazur, D. H. Reneker and B. M. Fanconni, *Pol. Comm.*, 28, 78 (1987).
68. R. G. Snyder, N. E. Schlotter, R. Alamo and L. Mandelkern, 19 (3), 621 (1986).
69. K. S. Lee, G. Wegner and S. L. Hsu, *Polymer*, 28, 889 (1987).
71. J. L. Koenig and M. K. Antoon, *J. Polym. Sci., Phys. Ed.*, 15, 1357 (1978).

72. S. B. Lin and J. L. Koenig, J. Pol. Sci., Phys. Ed., 20, 2277 (1980).
73. L. N. Orander, Opt. Spectrosc. (USSR), 11, 68 (1961).
74. J. B. Enns, Polym. Eng. Sci., 19, 756 (1979).
75. E. G. Boreio and J. L. Koenig, J. Chem. Phys., 52, 3425 (1970).
76. M. J. Hannon and J. Pol. Sci., A-2, 7, (1969).
77. Y. S. Huang and J. K. Koenig, J. Appl. Pol. Sci., 15, 1237 (1971).
78. W. Frank, H. Schmidt and W. Wuff, J. Pol. Sci., Polym. Symp. 61, 317 (1977).
79. W. Frank and W. Strohmeier, Prog. Colloid and Polym. Sci. 66, 205 (1979).
80. R. Bonart, L. Morbitzer and E. H. Muller, J. Macromol. Sci., Polym. Phys., B9, 447 (1974).
81. H. G. Zachmann and H. A. Stuart, Makromol. Chem., 44, 622 (1961).
82. T. Okada and L. Mandelkern, J. Pol. Sci., A2, 5, 239 (1967).
83. L. Mandelkern, Polym. J.(Tokyo), 17, 337 (1985).
84. M. Gavish and A. E. Woodward, Submitted.
85. P. Wang and A. E. Woodward, Makromol. Chem., in press.
86. F. J. Borio, PhD Dissertation; Case Western Reserve University; Cleveland, Ohio.

87. M. Gavish, P. Brennan and A. E. Woodward, *Macromolecules*, 21, 2075, (1988).
88. I. W. Levin, A. R. Pearce and W. C. Harris, *J. Chem. Phys.* 59, 3048 (1973).
89. I. W. Levin and A. R. Pearce, *J. Mol. Spec.* 49, 91 (1974).
90. J. Xu and A. E. Woodward, *Macromolecules*, 21, 83 (1988).
91. R. Criegee, B. Marchand and H. Wannwylus, *Justus Liebig Ann. Chem.*, 522, 99 (1942).
92. E. B. Wilson, Jr., J. C. Decius and P. C. Cross, *Molecular Vibrations* (Dover Publication, Inc. New York, 1980).
93. F. A. Cotton, *Chemical Applications of Group Theory* (Wiley Interscience, New York, 1971).
94. P. W. Higgs, *Proc. Roy. Soc. London*, A220, 472 (1953).
95. L. Piseri and G. Zerbi, *J. Chem. Phys.*, 48, 3561 (1968).
96. R. Criegee, *Justus Liebig Ann. Chem. Soc.*, 170 (1948).
97. J. W. Cook and R. Schoental, *J. Am. Chem. Soc.*, 170 (1948).
98. R. J. Fessenden and J. S. Fessenden, *Organic Chemistry*, (Willard Grand Press, Boston, Massachusetts, 1979).
99. J. W. Cook and R. Schoental, *Nature*, 161, 237 (1948).
100. G. M. Begder, *J. Chem. Soc.*, 456 (1949).
101. J. A. Elvidger and F. S. Spry, *J. Am. Chem. Soc.*, 2935 (1949).

102. B. M. Trost, L. Weber, P. E. Strege, T. J. Fulerton and T. J. Dietsche, *J. Am. Chem. Soc.*, 100, 3416 (1976).
103. F. C. Schilling, M. A. Gomez, A. E. Tonelli, F. E. Bovey and A. E. Woodward, *Macromolecules*, 20, 2954 (1987).
104. T. Uchida and H. Todokoro, *J. Pol. Sci. A2*, 5, 63 (1967).
105. H. D. Noether, C. G. Overberger and G. Halek, *J. Pol. Sci.*, A1, 7, 201 (1969).
106. H. D. Noether, *J. Pol. Sci.*, C, 16, 725 (1967).
107. G. Natta, P. Corradini and I. W. Bassini, *Nuovo Cimento Suppl.*, 15, 52 (1960).
108. A. Turner-Jones, *J. Pol. Sci.*, B, 1, 455 (1963).
109. H. Kakida, D. Makino, Y. Chatani, M. Kobayashi and H. Tokadoro, *Macromolecules*, 3, 569, (1970).
110. H. Tadokoro, Y. Takahashi, Y. Chatani and H. Kakida, *Makromol. Chem.*, 109, 96 (1967).
111. D. R. Holmes, C. W. Bunn and D. J. Smith, *J. Pol. Sci.*, 17, 159 (1955).
112. H. Arimoto, *J. Pol. Sci.*, A, 2, 2283 (1964).
113. G. Natta, L. Pasquon, P. Corradini, M. Peraldo and A. Zambelli, *Rend. Accad. Naz. Lincei.*, 28, 539 (1960).
114. G. Natta, M. Peraldo and G. Allegra, *Makromol. Chem.* 75, 215 (1964).
115. J. E. Mark, *J. Am. Chem. Soc.*, 89:26, 6829 (1968).

116. G. Ungar and S. J. Organ, *Plym. Rep.*, 28, 232 (1978).
117. F. C. Schilling, F. A. Bovey, A. E. Tonelli, J. Xu and A. E. Woodward, unpublished results.
118. I. Zemel and A. E. Woodward, Unpublished Results.
119. D. L. Pavia, G. M. Lampan and G. S. Kriz, Introduction to Spectroscopy, (Saunders College, Philadelphia, 1979).
120. J. M. Bhalerao, H. Rapoport, *J. Am. Chem. Soc.* 93, 4835, (1971).
121. R. L. Augustine, Oxidation, 1, 219 (Dekker, New York, 1971).
122. M. Bachhawat, N. K. Mathur, *Tet. Lett.*, 11, 691 (1971).
123. O. Perin-Roussel, F. Perin and P. Jacquignon, *Tet. Lett.*, 14, 1227, (1974).
124. M. Schroder, *Chem. Rev.*, 80, 187, (1980).
125. R. W. Freeksen, M. L. Raggio, C. A. Thoms and D. S. Watt, *Org. Chem*, 44, 702 (1979).
126. K. B. Sharpless and K. Akashi, *J. Am. Chem. Soc.*, 98:7, 1986 (1976).
127. W. P. Weber and J. P. Shepherd, *Tet. Lett.*, 12, 4907, (1972).
128. K. B. Wiberg and G. Foster, *J. Am. Chem. Soc.* 83, 423 (1961).
129. L. H. Sarett, *J. Am. Chem. Soc.* 70, 1454 (1948).
130. G. Berti, B. Macchia and F. Macchia, *Tet. Lett.*, 38, 3421, (1965).

131. Y. Tanaka, H. Sato and I. G. Gonzalez, *J. Pol. Sci., Polym. Chem. Ed.*, 17, 3027 (1979).
132. M. A. Golub and J. Heller, *Can. J. Chem*, 41, 937, (1963).
133. R. Ray and D. S. Matteson, *Tet. Lett.*, 21, 449 (1980)
134. M. Farina, The Stereochemistry of Linear Macromolecules, in E. L. Eliel and S. Wilen, Topics in Stereochemistry, 17, 1-96, (Weily and Sons, New York, 1987).
135. Y. Tanabe, R. G. Strohl, E. W. Fisher, *Polymer*, 27, 1147 (1986).
136. M. Moller, H-J. Cantow, H. Drotloff, D. Emies, K-S. Lee and G. Wegner, *Makromol. Chem.*, 187, 1237 (1986).
137. S. Krimm and J. Jakes, *Macromolecules*,4, 605 (1971).
138. H. H. Wills, *Polym. Comm.*, 28, 232 (1987).
139. P. C. Painter, J. Havens, W. W. Hart and J. L. Koenig *J. Pol. Sci., Polym. Phys. Ed.*, 15, 1223 (1977).
140. P. Wang and A. E. Woodward, *Macromolecules*, 20, 1818 (1987).
141. F. J. Borio and J. L. Koenig, *J. Chem. Phys.*, 52, 3425 (1970).
142. G. W. King, R. M. Hainer and O. McMahon, 20, 559 (1949).
143. M. Tasumi and S. Krimm, *J. Chem. Phys.*, 46, 755 (1967).
144. M. Gavish, J. Corrigan and A. E. Woodward, *Macromolecules*, 21, 2079, 1988.